NEUTRON STAR ZOO

SERGEI POPOV

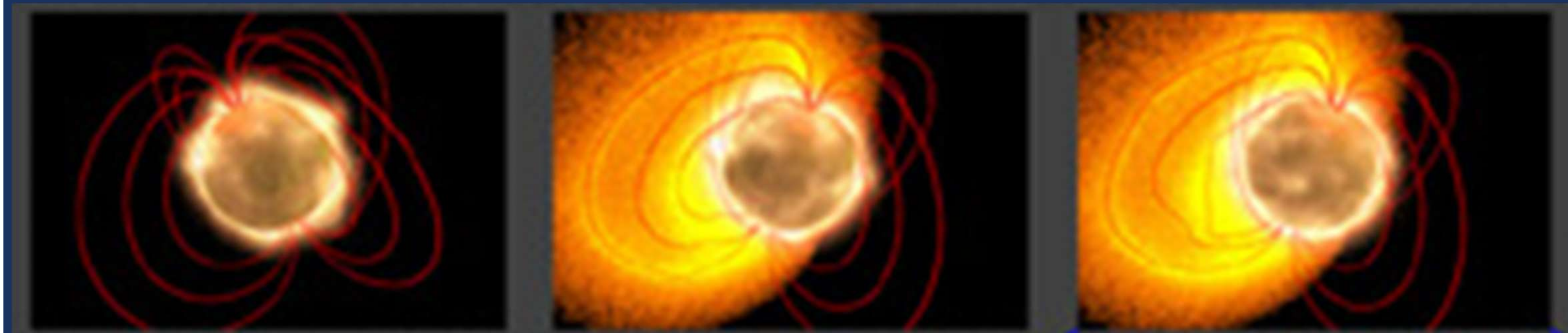

THE OLD ZOO: YOUNG PULSARS & OLD ACCRETORS

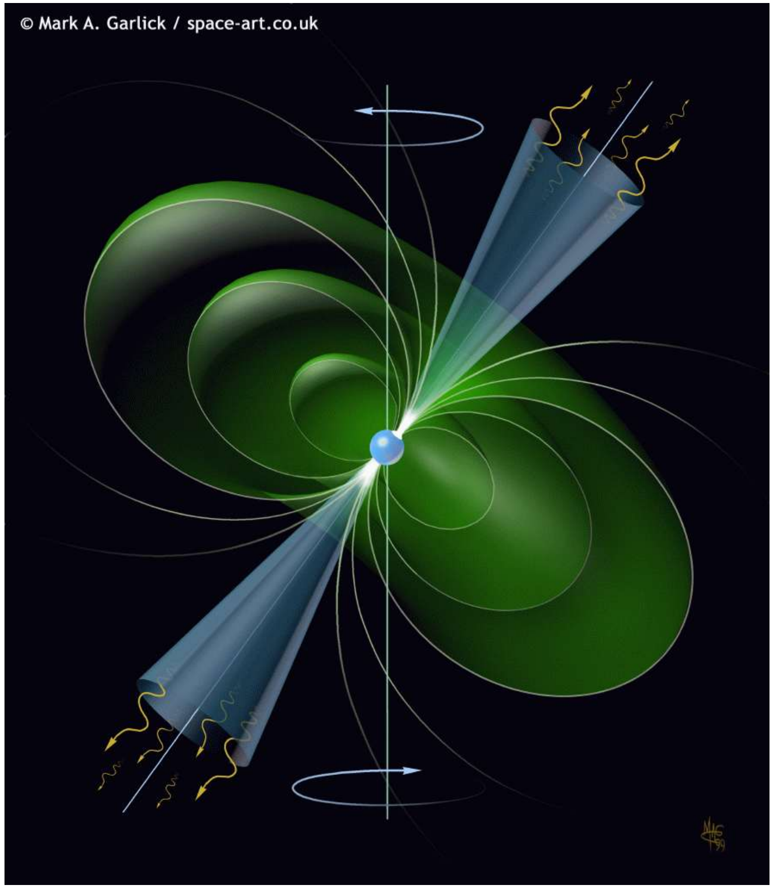

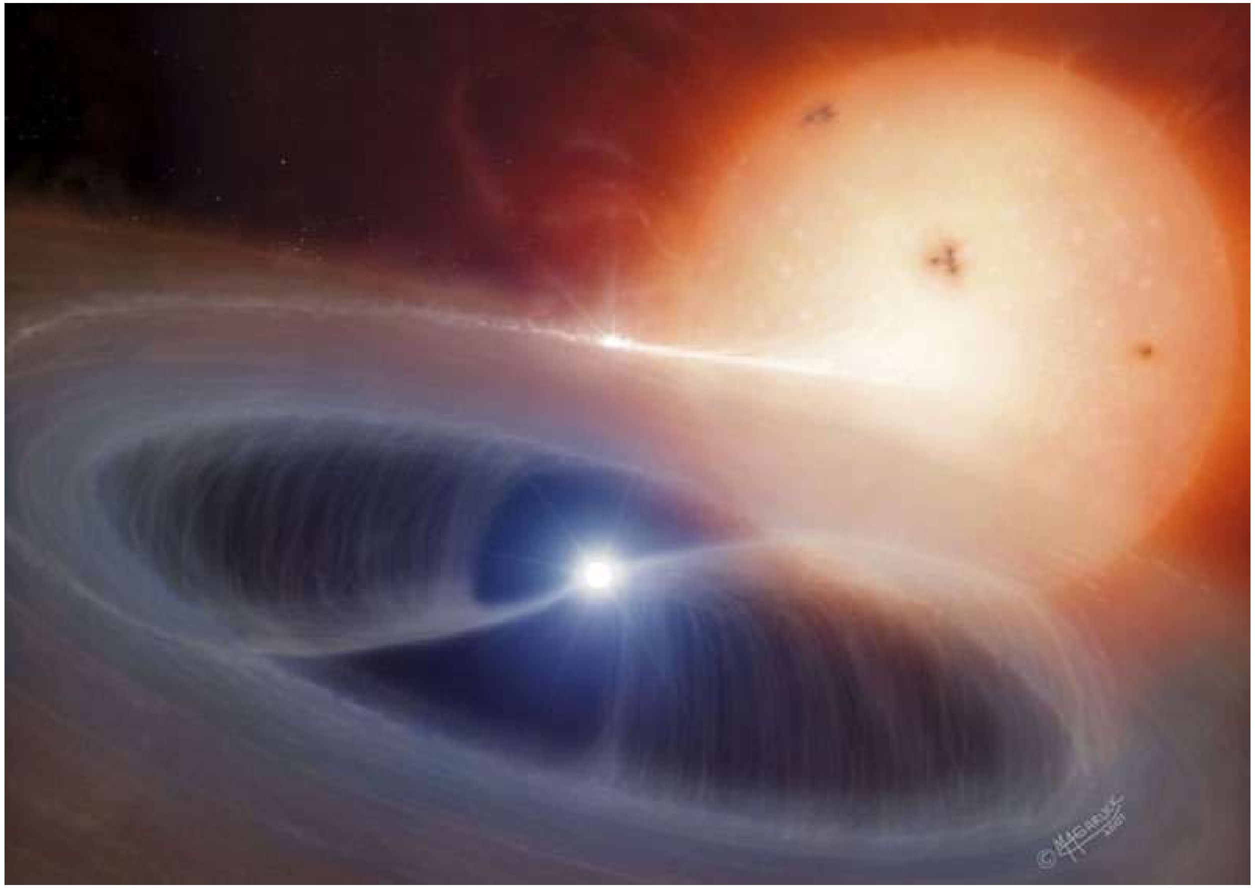

NSS IN THE MILKY WAY

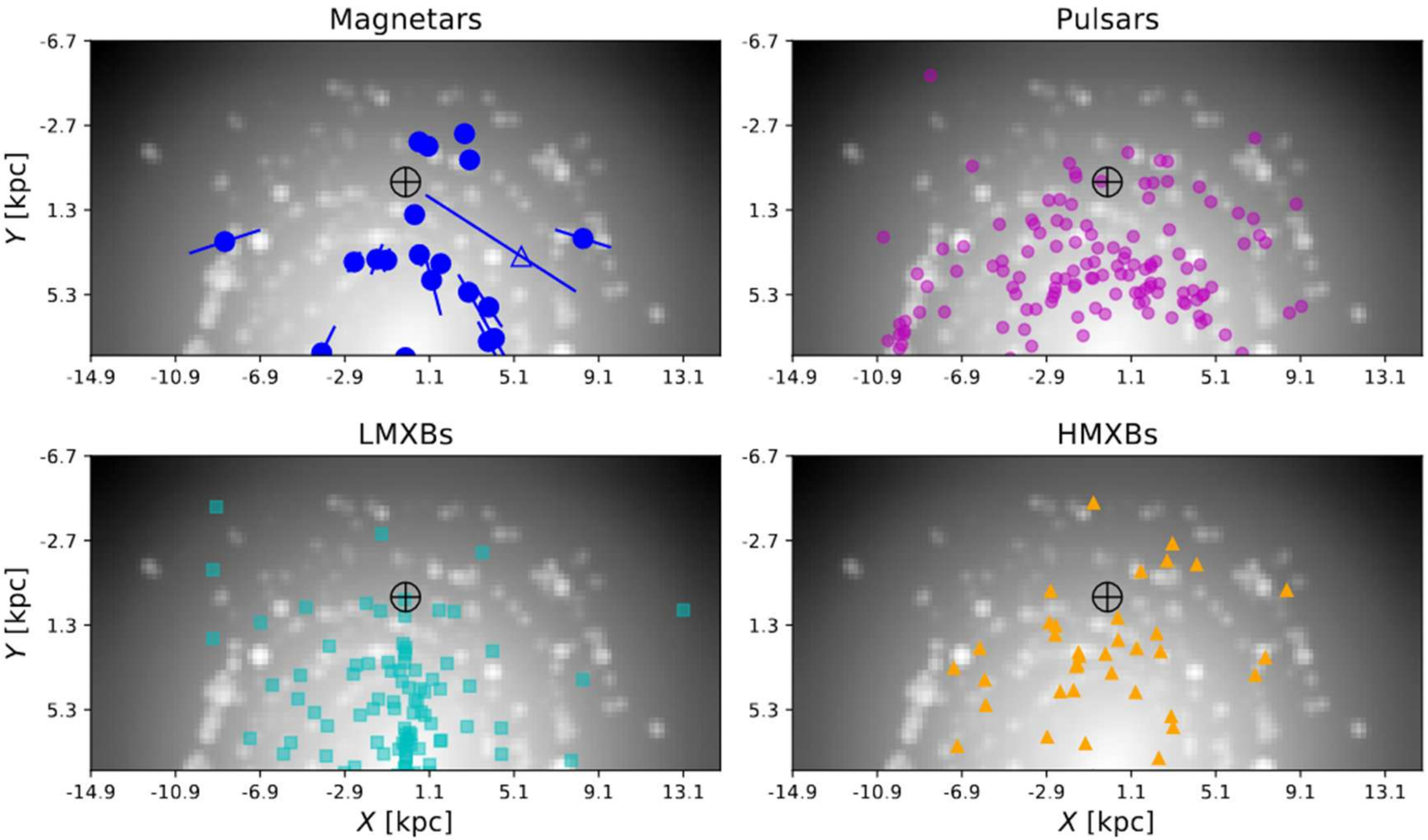

Young NSs are observed as isolated and binary sources.

Old NSs – mostly in binaries (LMXBs and mPSRs).

A new population of non-accreting NSs in binary systems is emerging thanks to Gaia observation and spectral analysis (LAMOST, etc.)

Do not forget also about isolated NSs discovered by the gravitational microlensing technique. New results will come from Gaia and Roman space telescope.

2105.04549

THE NEW ZOO OF YOUNG NEUTRON STARS

During last ~25-30 years it became clear that neutron stars can be born very different from each other.
In particular, absolutely non-similar to the Crab pulsar.

o High-B PSRs
o Compact central X-ray sources in supernova remnants
o Anomalous X-ray pulsars
o Soft gamma repeaters
o Transitional sources
o The Magnificent Seven
o Transient radio sources (RRATs)
o Long-period radio transients
o Sources of FRBs
o Magnetars in binaries

Old and new zoos: Harding arXiv:1302.0869

See a more recent review in 2306.02084

P-PDOT DIAGRAM

Some types of sources occupy specific regions of the P-Pdot diagram.
Some are more scattered, like RRATs.

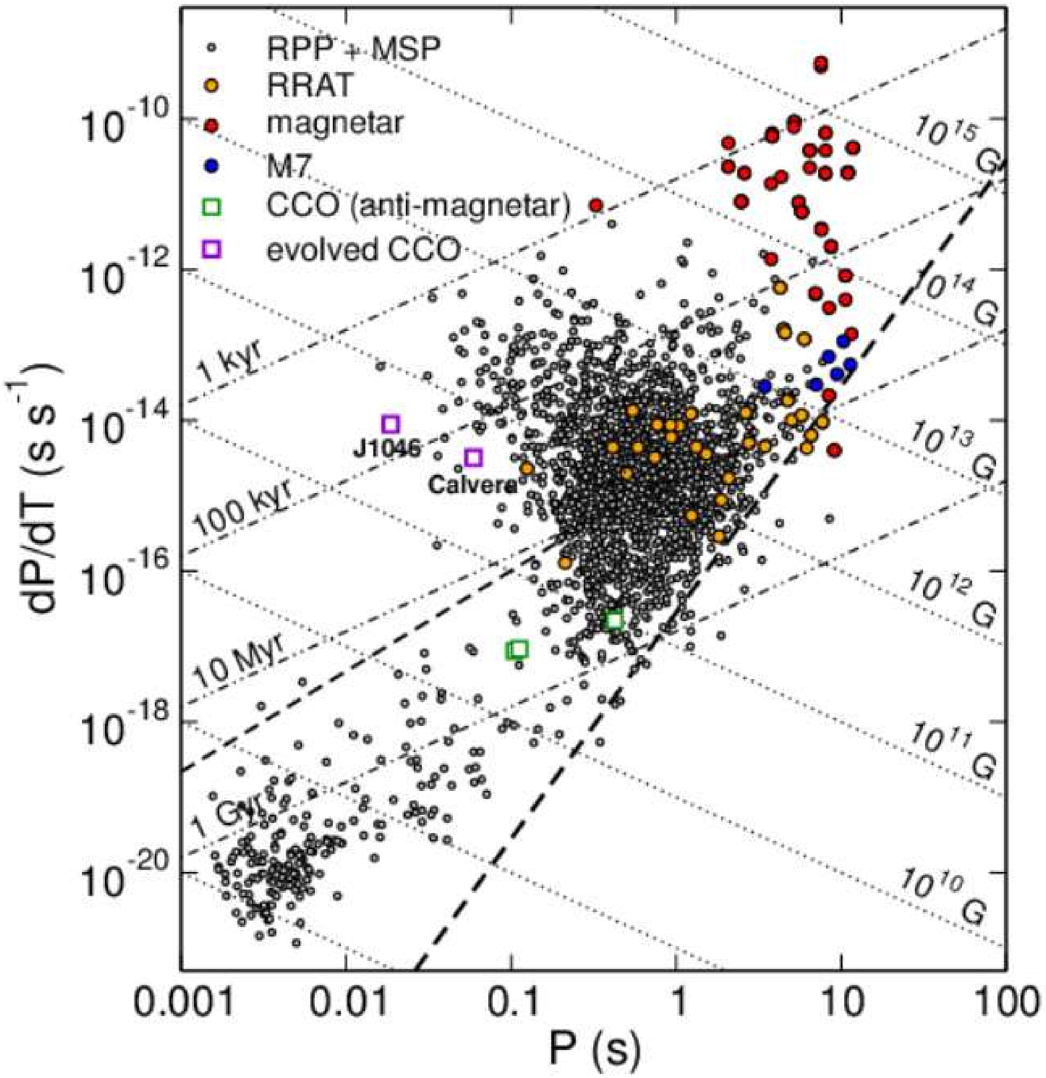

Pires et al. 2015

PULSARS

>3300 objects in the ATNF database

Plot: >2000 objects with
P>0.030 sec,
$B>10^{10}$G
which are not SGR/AXP/M7/RRATS
and are not in binaries.

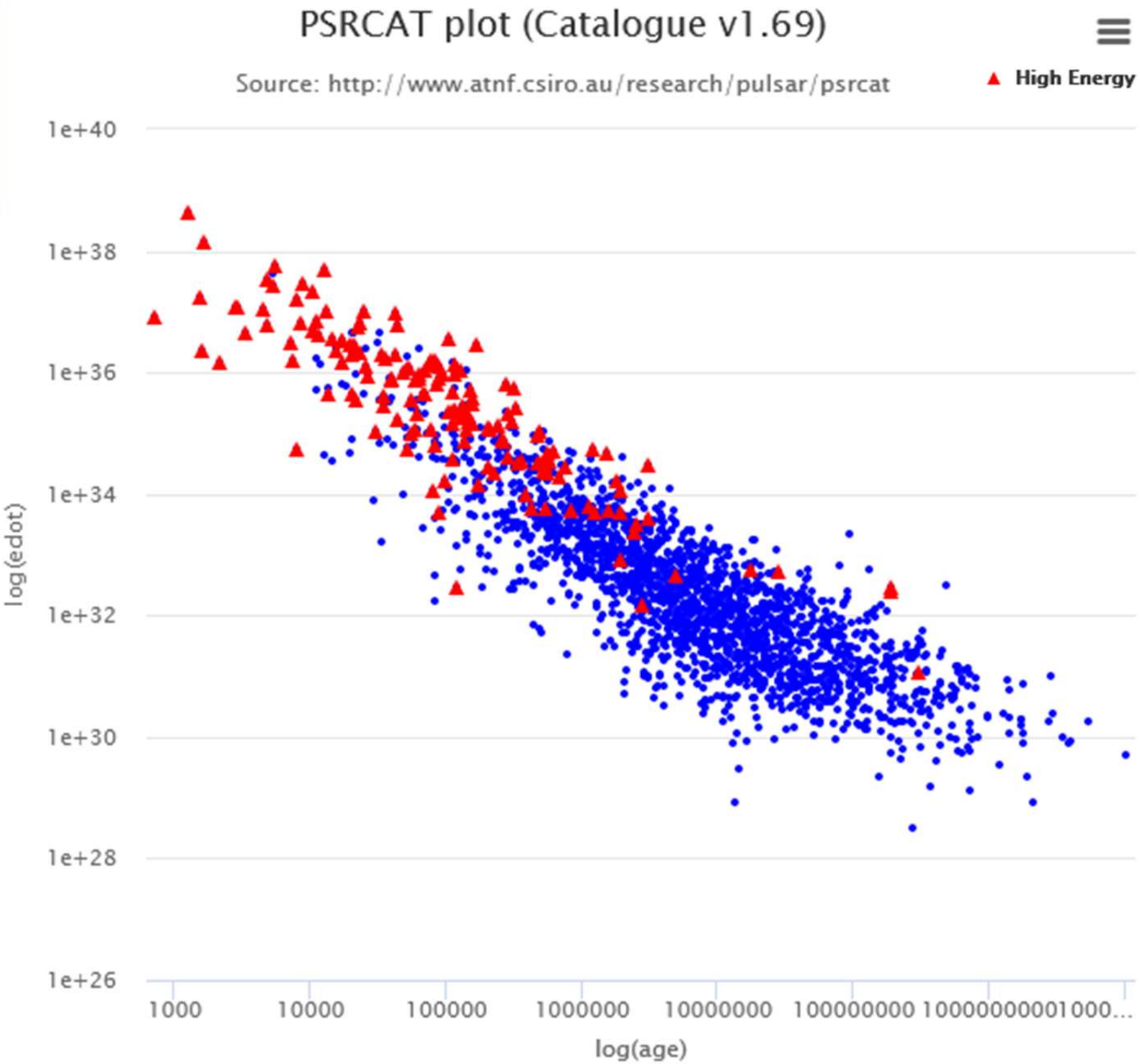

https://www.atnf.csiro.au/people/pulsar/psrcat/

COMPACT CENTRAL X-RAY SOURCES IN SUPERNOVA REMNANTS (CCOS)

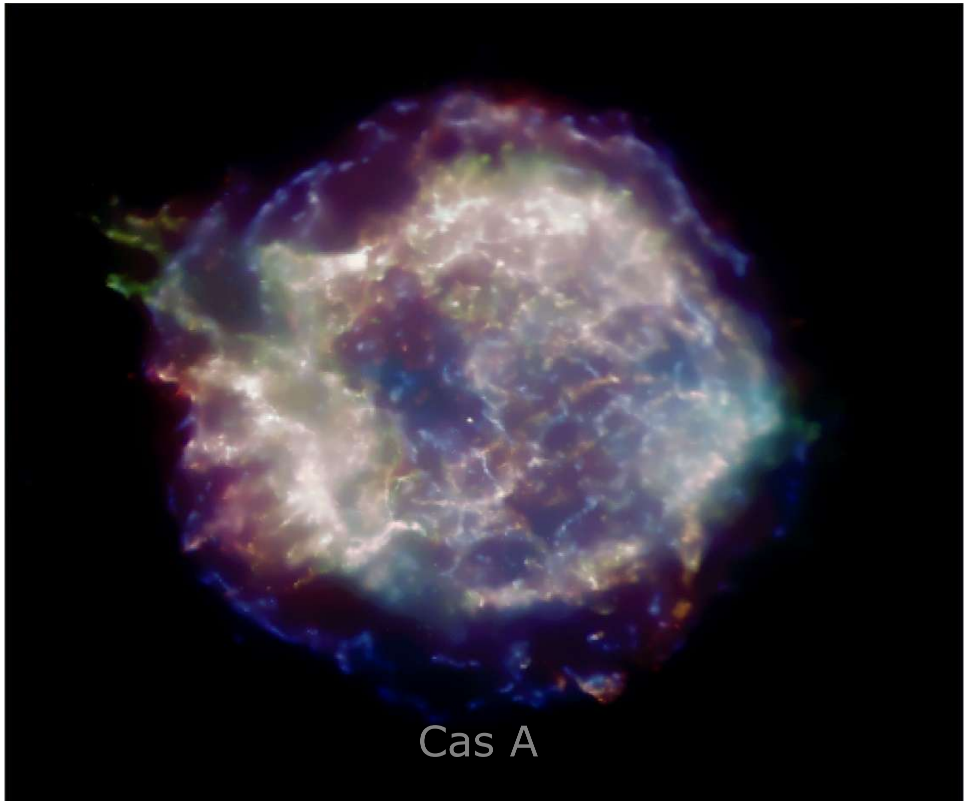

Rapid cooling
(Heinke et al. 1007.4719)

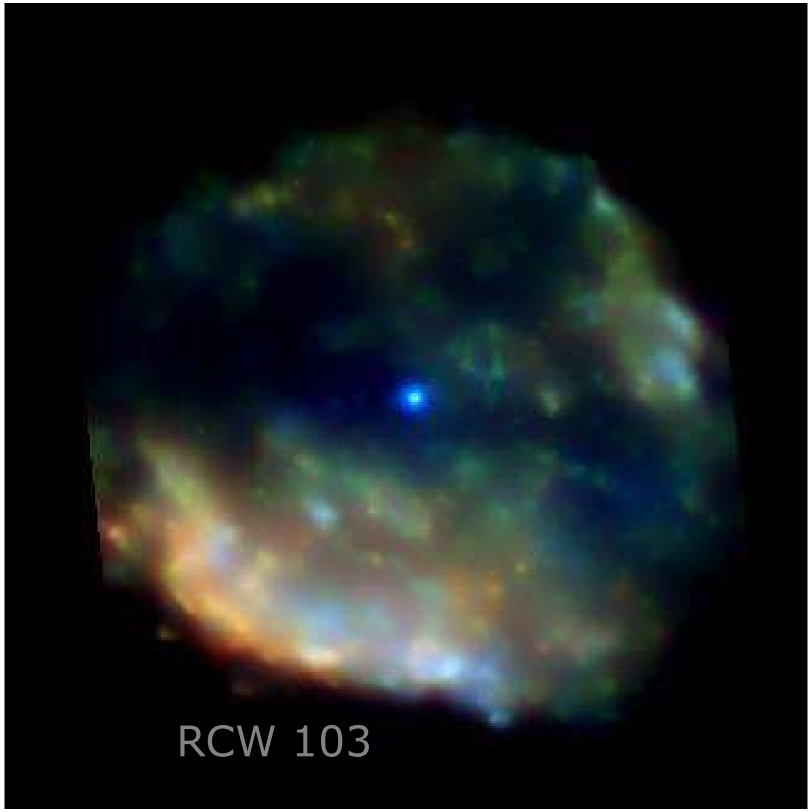

6.7 hour period
(de Luca et al. 2006)

CATALOGUE OF CCOS

CCO	SNR	SNR Age (kyr)	d (kpc)	P (s)	PF (%)	B_s (10^{10} G)	L_x bol (erg s^{-1})
RX J0822.0-4300	Puppis A	4.5	2.2	0.112	11	2.9	5.6×10^{33}
CXOU J085201.4-461753	G266.1-1.2	1	1	-	< 7	-	2.5×10^{32}
1E 1207.4-5209	PKS 1209-51/52	7	2.2	0.424	9	9.8	2.5×10^{33}
CXOU J160103.1-513353	G330.2+1.0	> 3	5	-	< 40	-	1.5×10^{33}
1WGA J1713.4-3949	G347.3-0.5	1.6	1.3	-	< 7	-	$\sim 1 \times 10^{33}$
XMMU J172054.5-372652	G350.1-0.3	0.9	4.5	-	-	-	3.9×10^{33}
XMMU J173203.3-344518	G353.6-0.7	~27	3.2	-	< 8	-	1.3×10^{34}
CXOU J181852.0-150213	G15.9+0.2	1–3	(8.5)	-	-	-	$\sim 1 \times 10^{33}$
CXOU J185238.6+004020	Kes 79	7	7	0.105	64	3.1	5.3×10^{33}
CXOU J232327.9+584842	Cas A	0.33	3.4	-	< 12	-	4.7×10^{33}

+ candidates + RCW103

http://www.iasf-milano.inaf.it/~deluca/cco/main.htm

MAGNETARS

1703.00068

McGill catalogue:
http://www.physics.mcgill.ca/~pulsar/magnetar/main.html

12 SGRs + candidates
12 AXPs + candidates
~30 objects

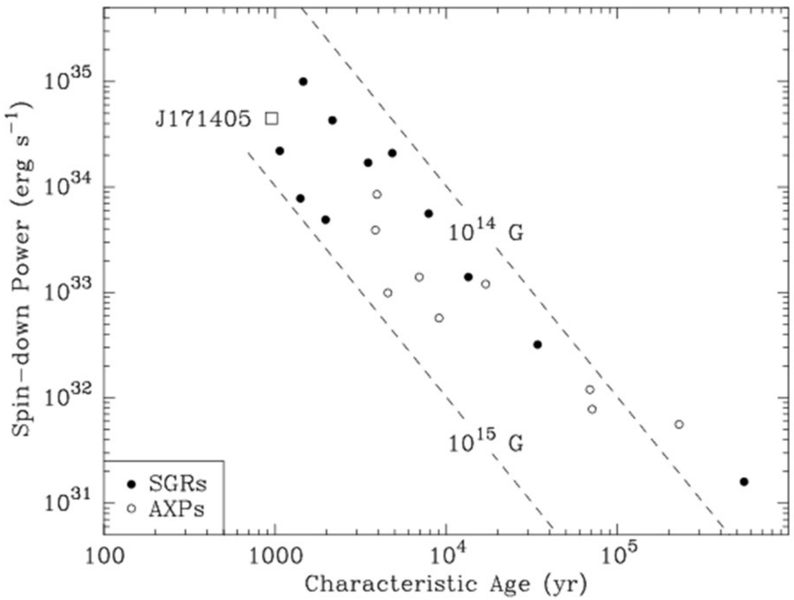

1907.13267

Name[b]	P (s)	B[c] (10^{14} G)	Age[d] (kyr)	$\dot{E}$[e] 10^{33} erg s^{-1}	D[f] (kpc)	L_X[g] 10^{33} erg s^{-1}
CXOU J010043.1-721134	8.02	3.9	6.8	1.4	62.4	65
4U 0142+61	8.69	1.3	68	0.12	3.6	105
SGR 0418+5729	9.08	0.06	36000	0.00021	~2	0.00096
SGR 0501+4516	5.76	1.9	15	1.2	~2	0.81
SGR 0526−66	8.05	5.6	3.4	2.9	53.6	189
1E 1048.1-5937	6.46	3.9	4.5	3.3	9.0	49
(PSR J1119−6127)	0.41	4.1	1.6	2300	8.4	0.2
1E 1547.0-5408	2.07	3.2	0.69	210	4.5	1.3
PSR J1622–4950	4.33	2.7	4.0	8.3	~9	0.4
SGR 1627−41	2.59	2.2	2.2	43	11	3.6
CXOU J164710.2–455216	10.6	<0.66	>420	<0.013	3.9	0.45
1RXS J170849.0–400910	11.01	4.7	9.0	0.58	3.8	42
CXOU J171405.7–381031	3.82	5.0	0.95	45	~13	56
SGR J1745–2900	3.76	2.3	4.3	10	8.3	<0.11
SGR 1806−20	7.55	20	0.24	45	8.7	163
XTE J1810–197	5.54	2.1	11	1.8	3.5	0.043
Swift J1822.3–1606	8.44	0.14	6300	0.0014	1.6	>0.0004
SGR 1833–0832	7.56	1.6	34	0.32	...	...
Swift J1834.9–0846	2.48	1.4	4.9	21	4.2	<0.0084
1E 1841–045	11.79	7.0	4.6	0.99	8.5	184
(PSR J1846−0258)	0.327	0.49	0.73	8100	6.0	19
3XMM J185246.6+003317	11.56	< 0.41	> 1300	< 0.0036	~7	< 0.006
SGR 1900+14	5.20	7.0	0.9	26	12.5	90
SGR 1935+2154	3.24	2.2	3.6	17	...	...
1E 2259+586	6.98	0.59	230	0.056	3.2	17

EXTRAGALACTIC HYPERFLARES OF MAGNETARS

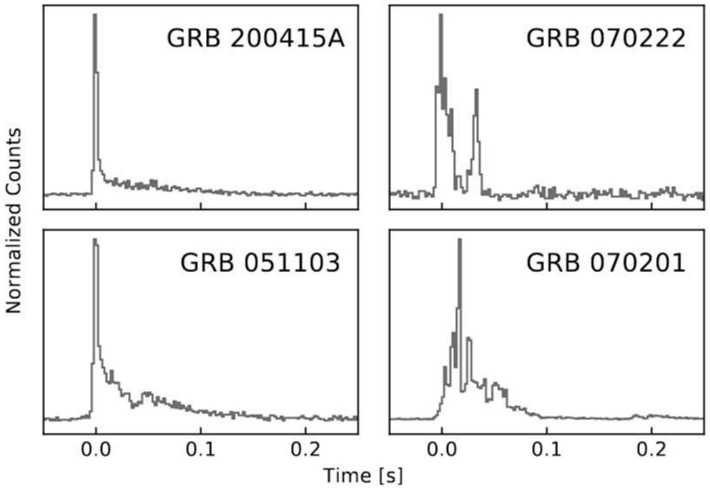

	Known			Extragalactic			
MGF Event	790305B	980827	041227	200415A	070222	051103	070201
Origin							
False Alarm Rate	0	0	0	4.9×10^{-6}	7.8×10^{-6}	1.5×10^{-5}	1.2×10^{-4}
BNS Excl. [Mpc]					6.7	5.2	3.5
Galaxy Properties							
Catalog Name	LMC	MW	MW	NGC253	M83	M82	M31
Distance [Mpc]	0.054	0.0125	0.0087	3.5	4.5	3.7	0.78
SFR [$M_\odot/yr$]	0.56	1.65	1.65	4.9	4.2	7.1	0.4
GRB Properties							
Duration [s]	<0.25	<1.0	<0.2	0.100	0.038	0.138	0.010
Rise Time [ms]	~2	~4	~1	2	4	2	24
$L_{\rm iso}^{Max}$ [10^{46} erg/s]	0.65	2.3	35	140	40	180	12
$E_{\rm iso}$ [10^{45} erg]	0.7	0.43	23	13	6.2	53	1.6
Index			-0.7	0.0	-1.0	-0.2	-0.6
$E_{\rm peak}$ [keV]	500	1200	850	1080	1290	2150	280

Four hyperflares of SGRs
are identified in near-by galaxies.

Among sGRBs there might be more
events of this type, but it is
very difficult to identify them.

2101.05144

THE MAGNIFICENT SEVEN

Name	Period, s
RX 1856	7.05
RX 0720	8.39
RBS 1223	10.31
RBS 1556	------
RX 0806	11.37
RX 0420	3.45
RBS 1774	9.44

Radioquiet
Near-by
Thermal emission
Long periods
Absorption features

PROPERTIES OF THE MAGNIFICENT SEVEN

1401.7147

Object	kT_∞ (eV)	P (s)	p_f (%)	$\log(\dot{P})$ (s s^{-1})	$\log(\dot{E})$ (erg s^{-1})	$\log(\tau_{ch})$ (yr)	$\log(t_{kin})$ (yr)	$\log(B_{dip})$ (10^{13} G)	$\log(B_{cyc})$ (10^{13} G)	Reference
RX J1856.5-3754	61	7.06	1	−13.527	30.580	6.58	5.62	13.17	–	[1]
RX J0720.4-3125	84 – 93	8.39	11	−13.156	30.726	6.28	5.93	13.39	13.75	[2]
RX J1605.3+3249	100	~~3.39~~	4	−11.796	33.267	4.53	5.65	13.87	13.92	[3]
RX J1308.6+2127	100	10.31	18	−12.951	30.663	6.16	5.95	13.54	13.60	[4]
RX J2143.0+0654	104	9.43	4	−13.398	30.332	6.57	–	13.29	14.15	[5]
RX J0806.4-4123	95	11.37	6	−13.260	30.227	6.51	–	13.40	13.96	[6]
RX J0420.0-5022	48	3.45	17	−13.553	31.487	6.29	–	13.00	–	[7]

0907.0054

XDINS	Pulsed emission			Bursty emission		
	S_{lim} (μJy)	$L_{1400}^{p,max}$ (mJy kpc^2)	$L_{820}^{p,max}$ (mJy kpc^2)	rate upper limit (hr^{-1})	S_{lim}^{sp} (mJy)	$L_{1400}^{b,max}$ (mJy kpc^2)
RX J0720.4−3125	8	4×10^{-4}	10^{-3}	0.25	21	1
RX J0806.4−4123	10	4×10^{-3}	10^{-2}	0.32	18	6.9
RX J1308.6+2127	10	4×10^{-3}	10^{-2}	0.24	17	6.5
RX J1605.3+3249	8	3×10^{-3}	8×10^{-3}	0.25	22	8.4
RX J1856.5−3754	14	1.4×10^{-4}	3.6×10^{-4}	0.32	24	0.2
RX J2143.0+0654	13	5×10^{-3}	1.3×10^{-2}	0.36	20	7.6

About a few new candidates see Kurpas et al. (2006) and references therein.

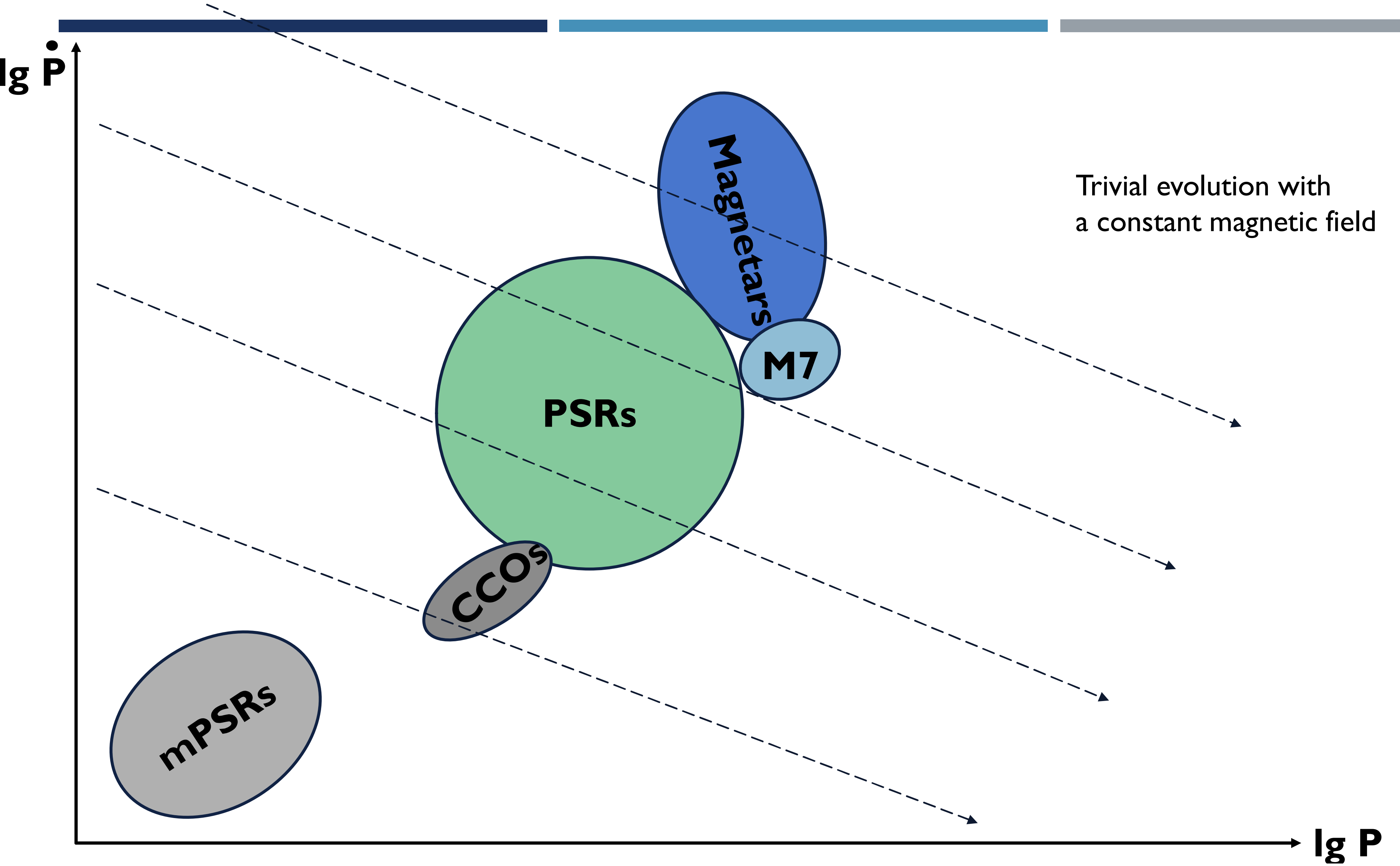
lg Ṗ
Magnetars
Trivial evolution with
a constant magnetic field
M7
PSRs
CCOs
mPSRs
lg P

TOO MANY NSS???

Keane, Kramer 2008, arXiv: 0810.1512

$\beta_{\rm PSR}$, $n_{\rm e}$	PSRs	RRATs	XDINSs	Magnetars	Total	CCSN rate
FK06, NE2001	2.8 ± 0.5	$5.6^{+4.3}_{-3.3}$	2.1 ± 1.0	$0.3^{+1.2}_{-0.2}$	$10.8^{+7.0}_{-5.0}$	1.9 ± 1.1
L+06, NE2001	1.4 ± 0.2	$2.8^{+1.6}_{-1.6}$	2.1 ± 1.0	$0.3^{+1.2}_{-0.2}$	$6.6^{+4.0}_{-3.0}$	1.9 ± 1.1
L+06, TC93	1.1 ± 0.2	$2.2^{+1.7}_{-1.3}$	2.1 ± 1.0	$0.3^{+1.2}_{-0.2}$	$5.7^{+4.1}_{-2.7}$	1.9 ± 1.1
V+04, NE2001	1.6 ± 0.3	$3.2^{+2.5}_{-1.9}$	2.1 ± 1.0	$0.3^{+1.2}_{-0.2}$	$7.2^{+5.0}_{-3.4}$	1.9 ± 1.1
V+04, TC93	1.1 ± 0.2	$2.2^{+1.7}_{-1.3}$	2.1 ± 1.0	$0.3^{+1.2}_{-0.2}$	$5.7^{+4.1}_{-2.7}$	1.9 ± 1.1

It seems, that the total birth rate is larger than the rate of CCSN.

Note, that the authors do not include CCOs
(but may be now RRATs can be excluded as a separate class).

So, either some estimates are wrong,
or some sources evolve into others.

GRAND UNIFICATION: 1005.0876

TRANSIENT RADIOPULSAR

PSR J1846-0258
P=0.326 sec
B=5 10^{13} G

However,
no radio emission
detected.
Due to beaming?

Among all rotation powered
PSRs it has the largest Edot.
The smallest spindown age (884 yrs).

The pulsar increased
its luminosity in X-rays.
Increase of pulsed X-ray flux.
Magnetar-like X-ray bursts (RXTE).
Timing noise.

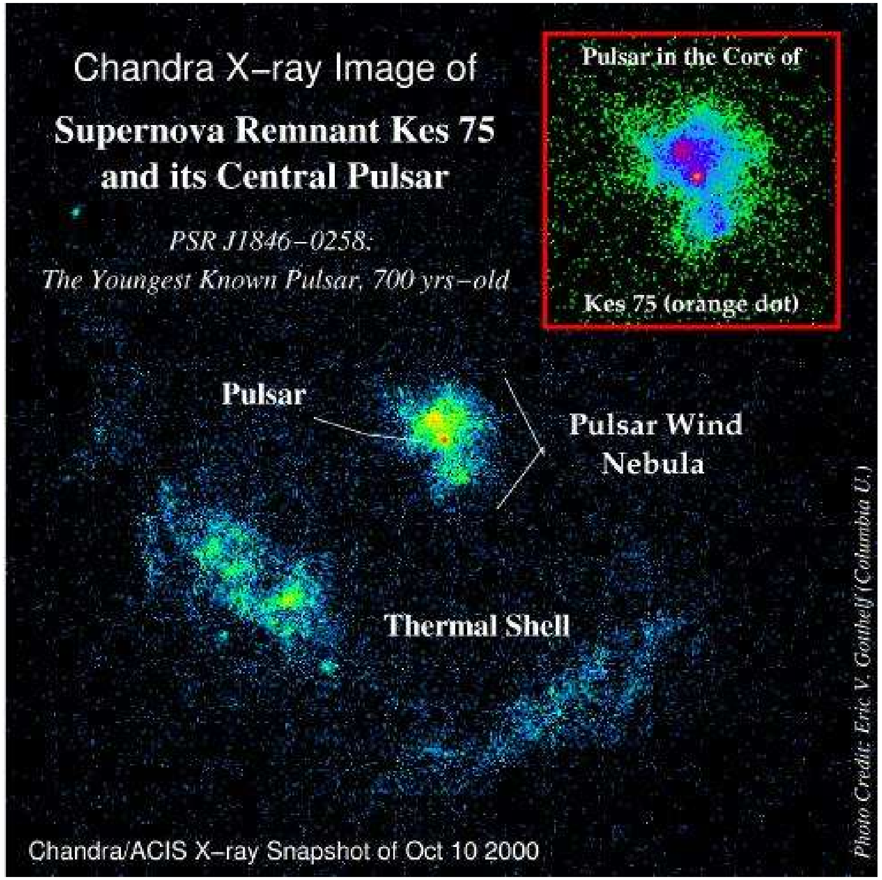

0802.1242, 0802.1704

Gavriil et al. 0802.1704

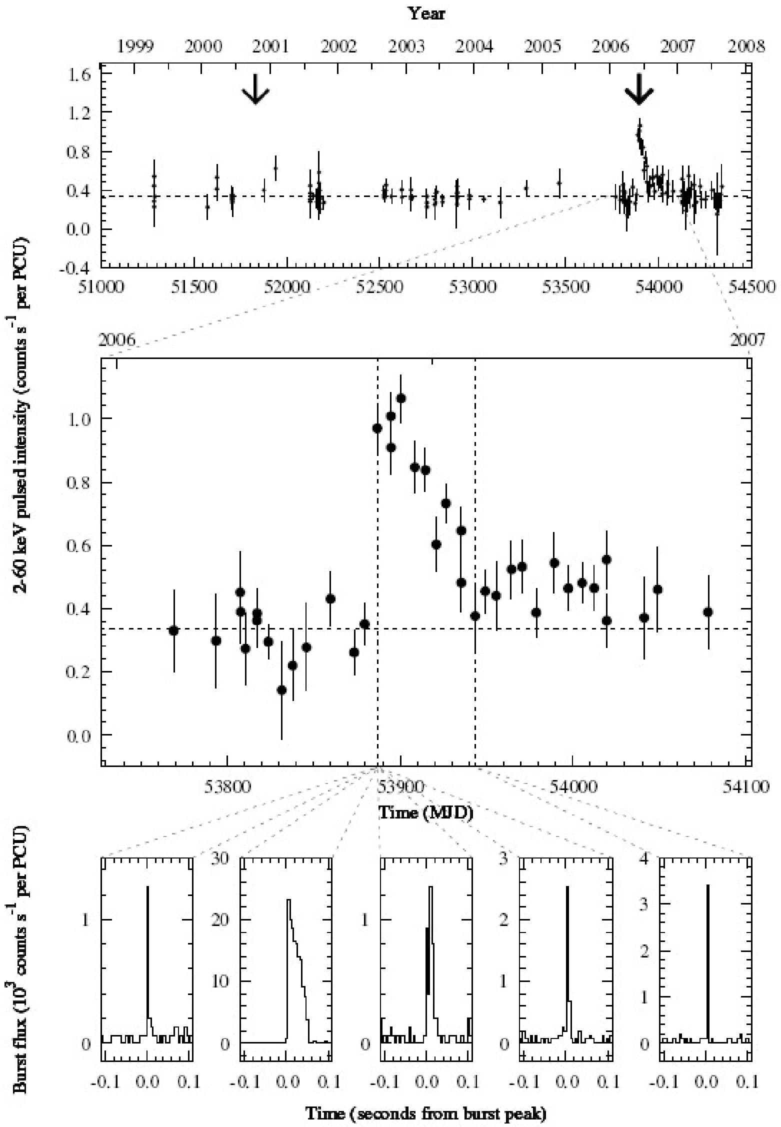

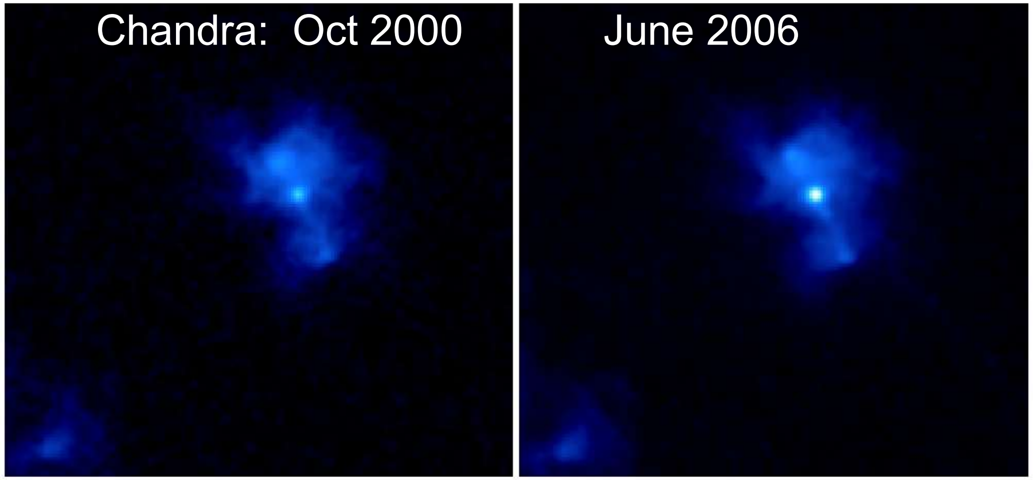

Table 1 PSR J1846−0258 Burst Temporal and Spectral Properties

	Burst 1	Burst 2	Burst 3	Burst 4	Burst 5
Temporal properties					
Burst day (MJD)	53886	53886	53886	53886	53943
Burst start time (fraction of day)	0.92113966(5)	0.93247134(1)	0.93908845(2)	0.94248467(5)	0.45543551(1)
Rise time, t_r (ms)	$4.2^{+3.5}_{-2.0}$	$1.1^{+0.9}_{-0.5}$	$1.90^{+1.7}_{-0.9}$	$4.1^{+3.1}_{-1.9}$	$0.9^{+2.2}_{-0.7}$
T_{90} (ms)	$71.8^{+38.0}_{-5.5}$	$42.9^{+0.3}_{-0.2}$	$137.0^{+11.4}_{-36.2}$	$33.4^{+29.1}_{-23.1}$	$65.3^{+0.7}_{-0.5}$
Phase (cycles)	-0.49(1)	-0.04(1)	-0.20(1)	-0.05(1)	-0.08(1)
Fluences and fluxes					
T_{90} Fluence (counts/PCU)	8.9±0.7	712.8±2.5	18.3±0.7	18.4±0.7	18.4±1.1
T_{90} Fluence (10^{-10} erg/cm^2)	4.1±2.4	289.9±13.1	6.6±2.5	5.8±1.7	5.3±2.0
Flux for 64 ms (10^{-10} erg/s/cm^2)	57±36	4533±227	99±41	97±31	79±32
Flux for t_r (10^{-10} erg/s/cm^2)	678±427	5783±885	810±385	828±284	2698±1193
Spectral properties					
Power-law index	0.89±0.58	1.05±.04	1.14±0.34	1.36±0.25	1.41±0.31
χ^2/DoF (DoF)	0.42 (1)	1.16 (55)	0.97 (3)	0.35 (2)	1.18 (2)

RCW103 – A SPECIAL KIND OF A MAGNETAR

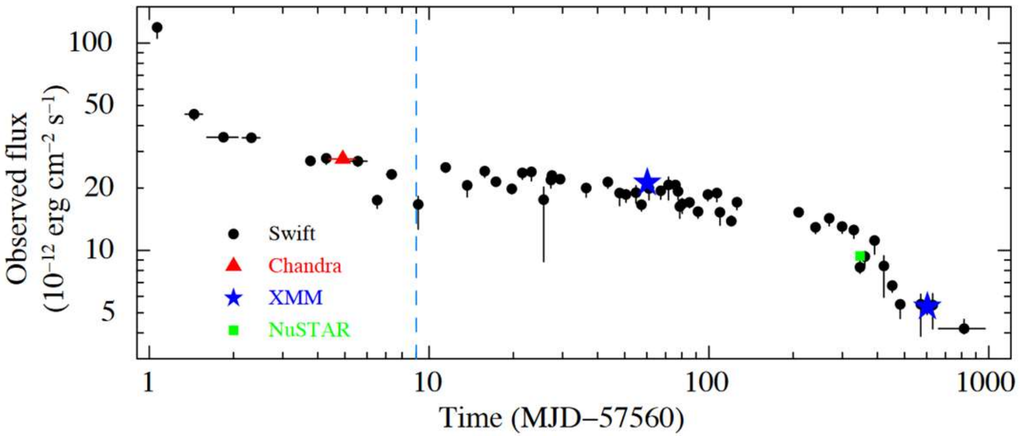

1904.05424

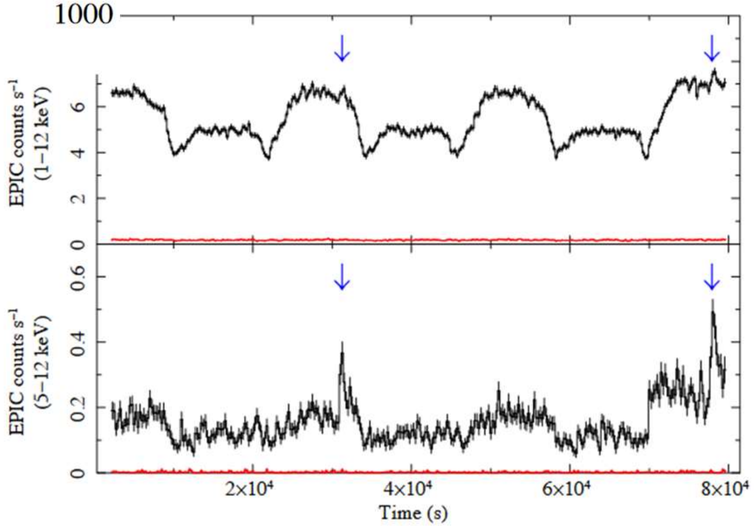

Looked like a CCO.

6.7 hours spin period!

SGR-like bursts.

CRUSTAL ENERGY RELEASE IN RCW103

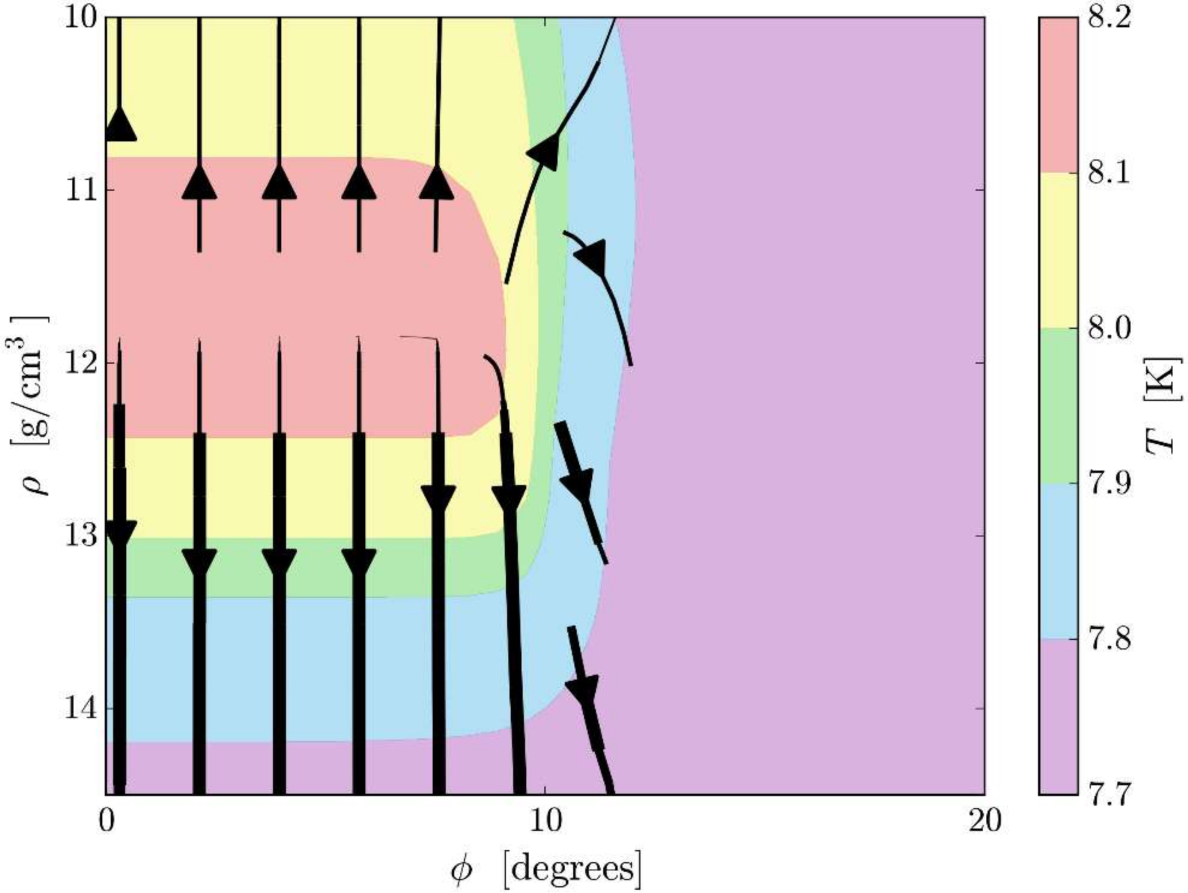

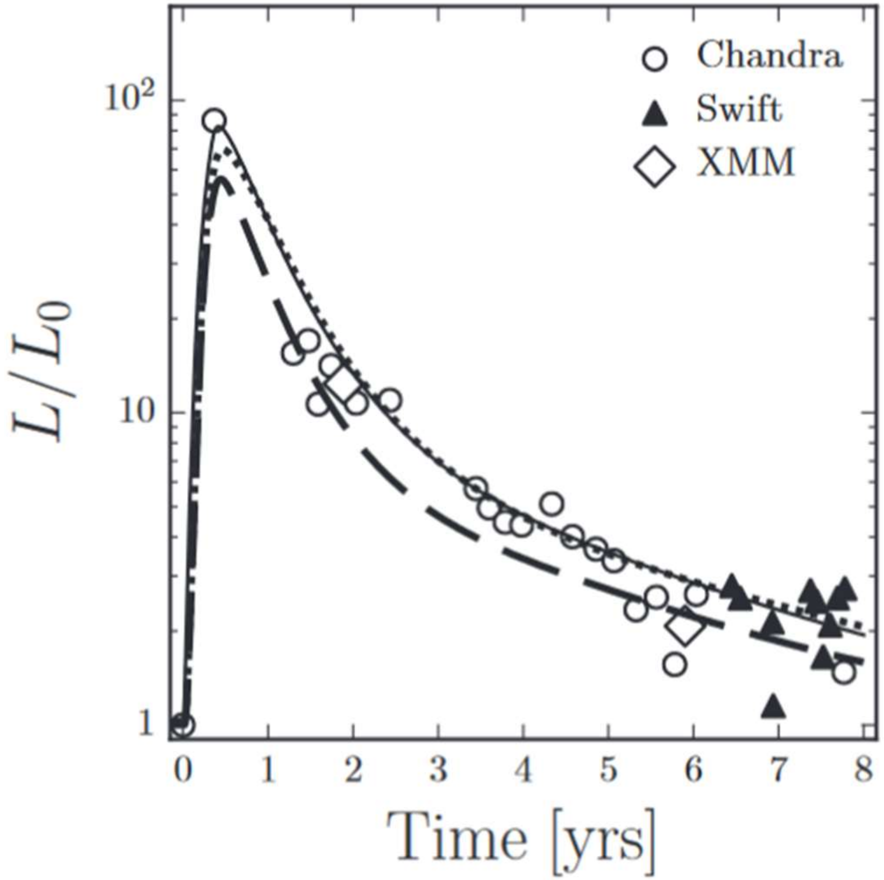

1504.03279

QUIESCENT MAGNETAR J1622–4950

Normally, magnetars are detected via their strong activity: gamma-ray bursts or enhanced X-ray luminosity.

This one was detected in radio observations
The field is estimated to be $B \sim 3\ 10^{14}$ G

It seems to be the first magnetar to be detected in a quiescent state.

PSR J1622–4950 was detected in a radio survey
As a pulsar with P=4.3 s.

Noisy behavior in radio

See reviews on high-B PSRs in 1010.4592, 1805.01680

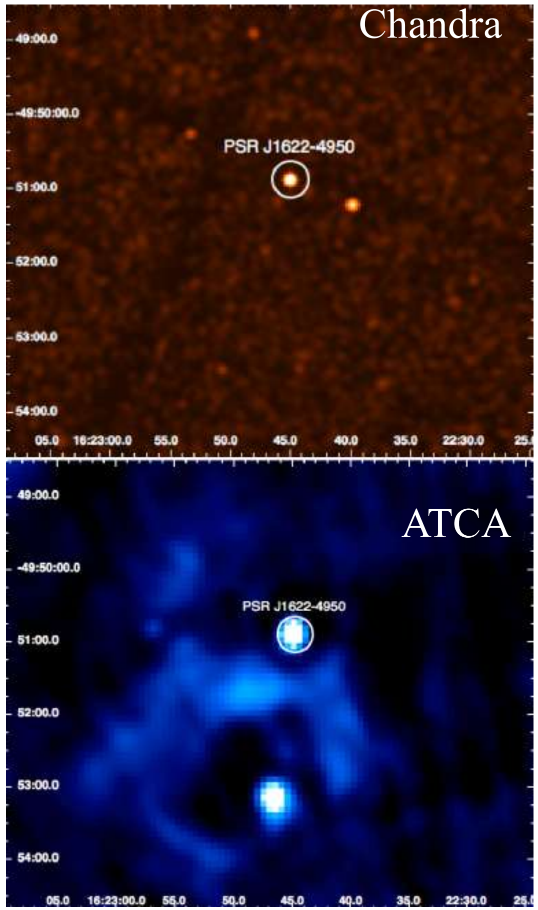

arXiv: 1007.1052

REVIVAL OF J1622–4950

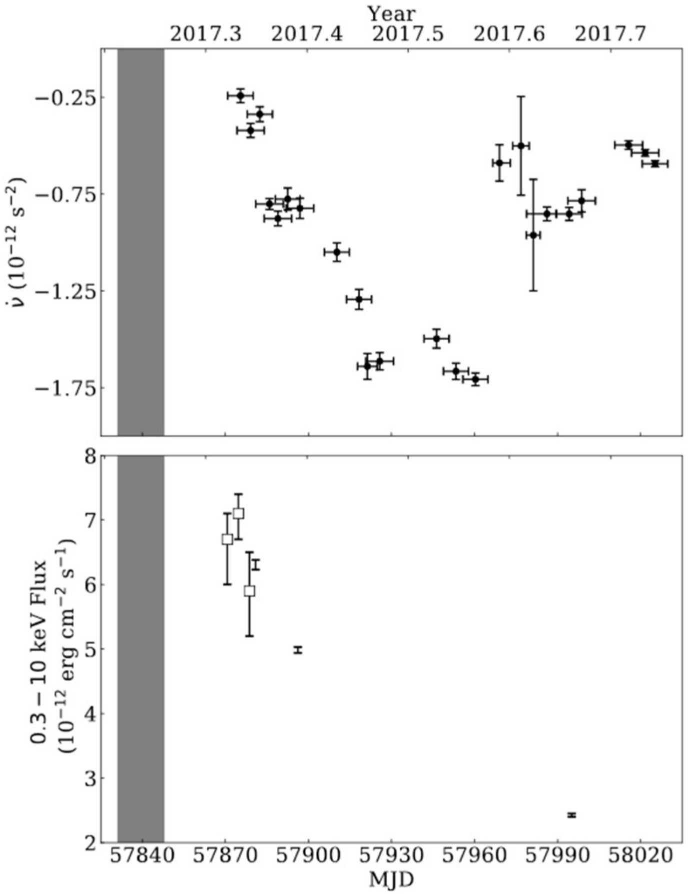

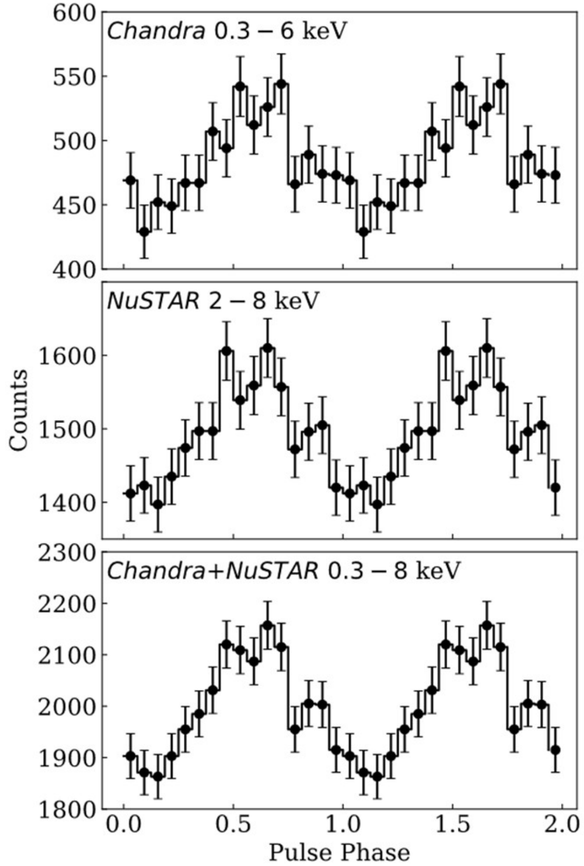

1804.01933

Before the revival the
X-ray flux was decaying
for several years.
Probably, the source
has been active years before.

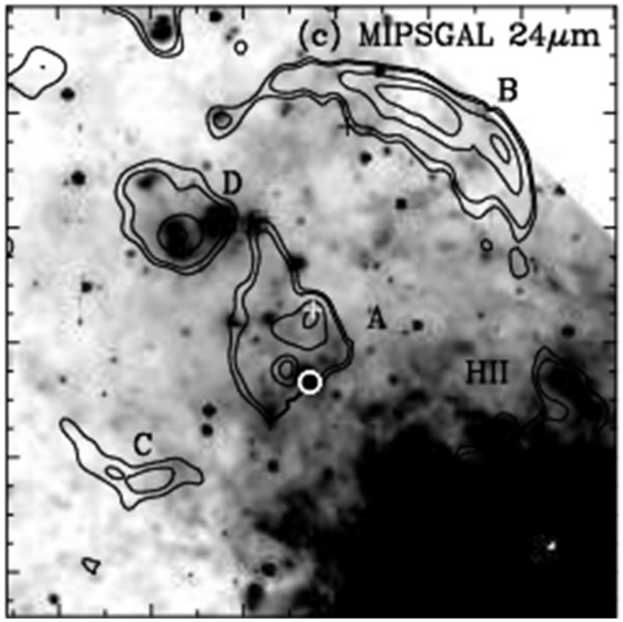

SNR G333.9+0.0

FALLBACK AND FIELD RE-EMERGENCE

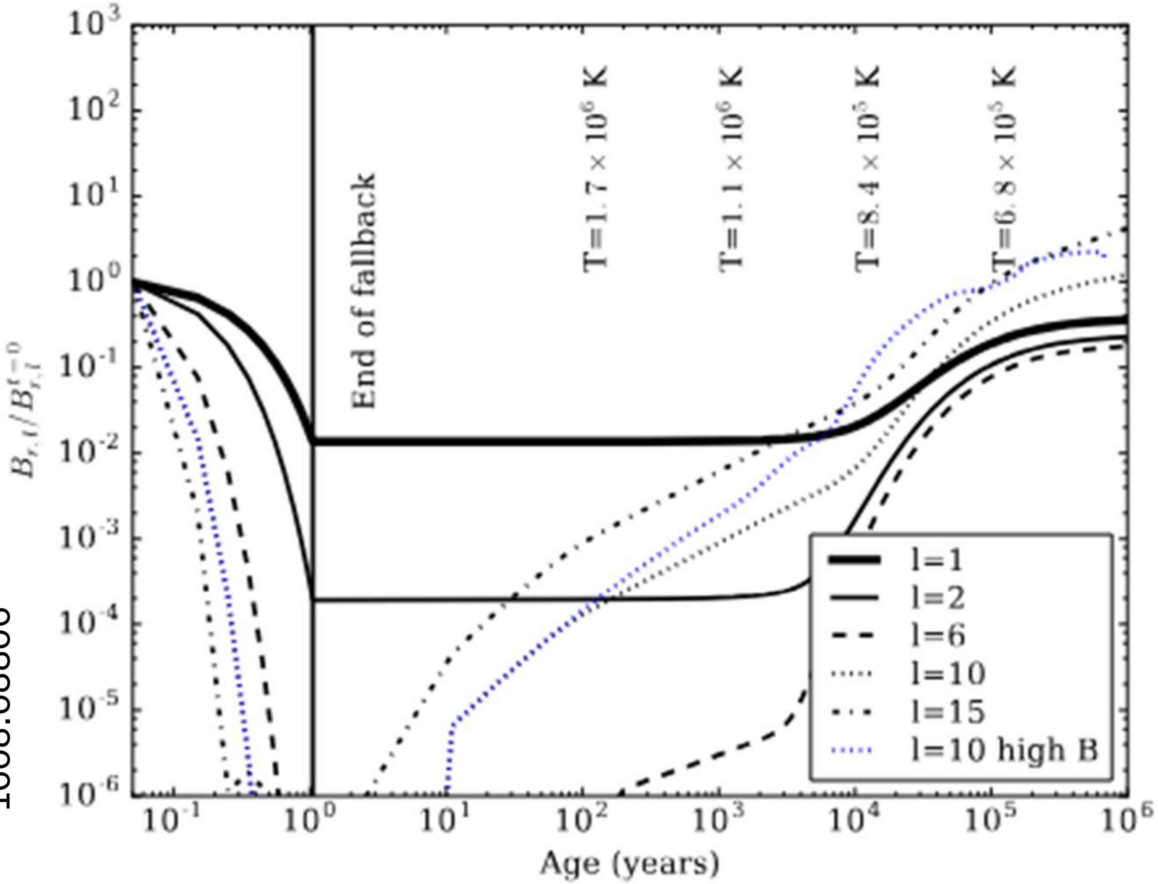

1608.08806

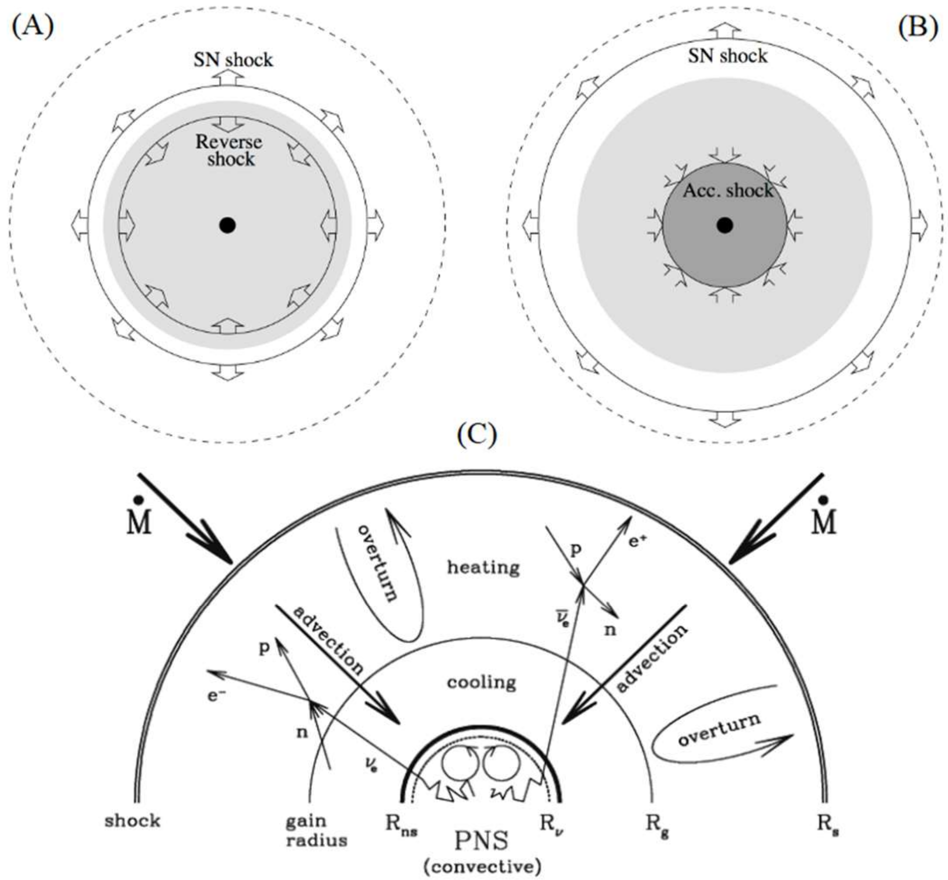

1809.07057

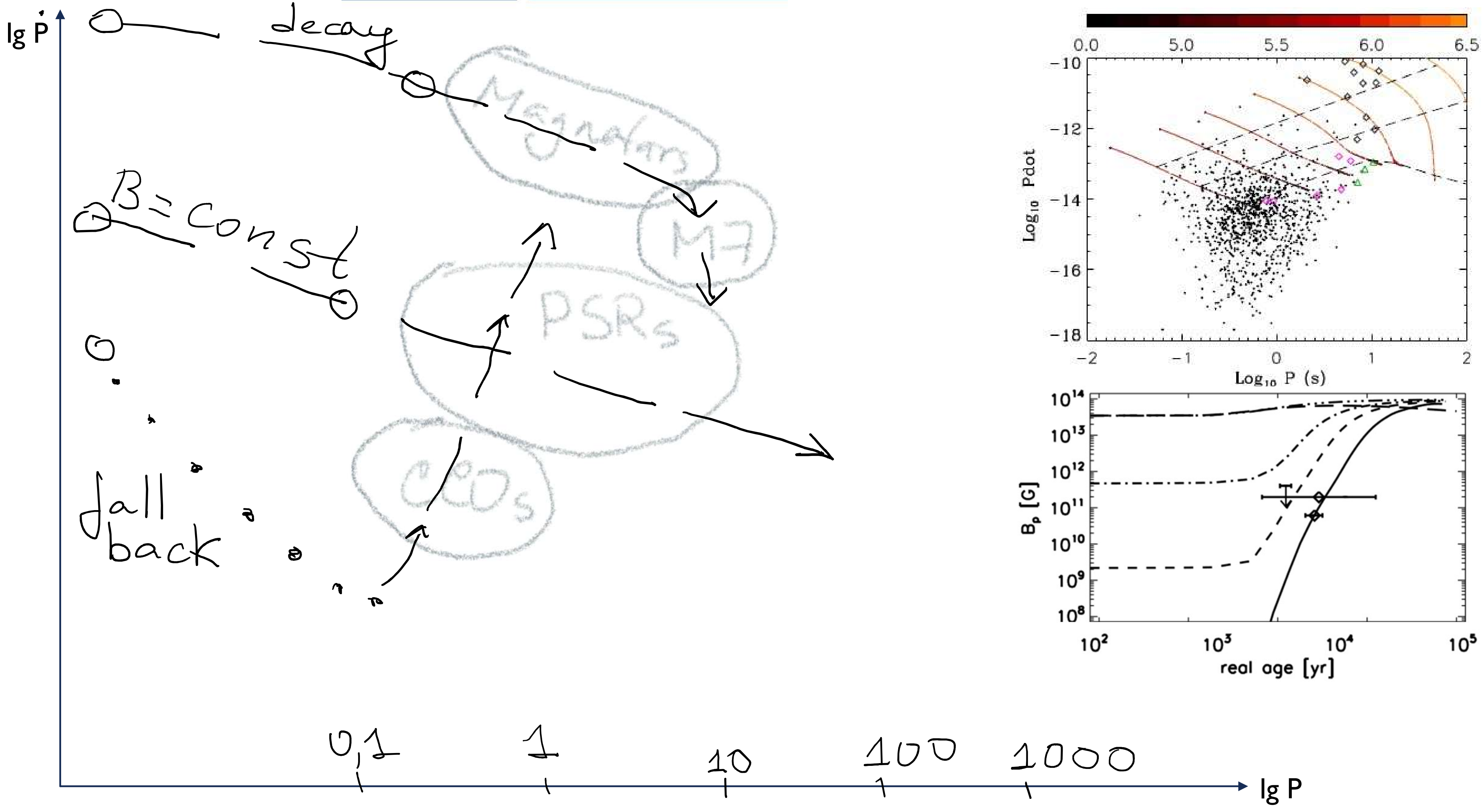

Popov et al. MNRAS 2010

1206.2014

"HIDDEN" MAGNETARS

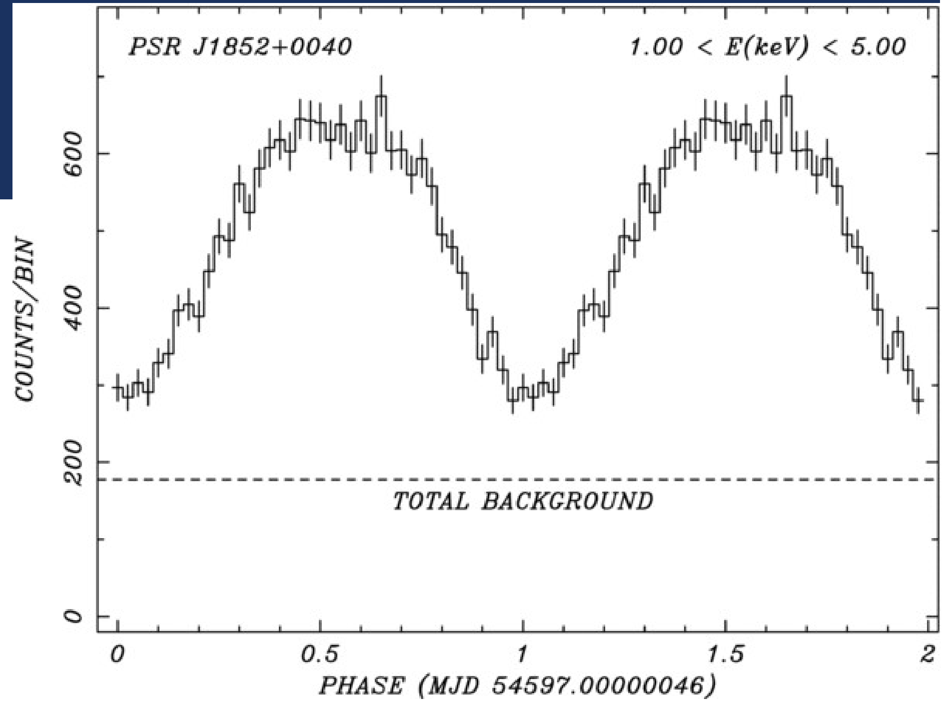

Halpern, Gotthelf 2010

Kes 79. PSR J1852+0040. P~0.1 s

Shabaltas & Lai (2012) show that large pulse fraction of the NS in Kes 79 can be explained if its magnetic field in the crust is very strong: few $\times 10^{14}$ G.

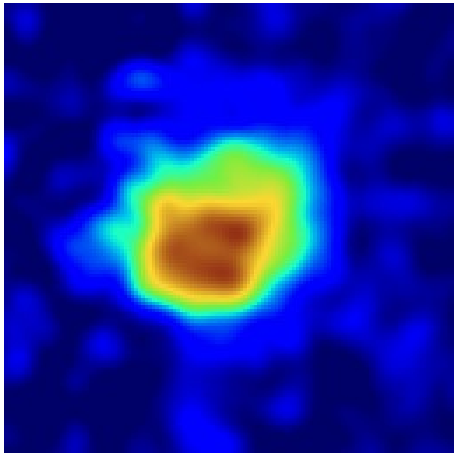

Kes 79

- If submergence of the field happens rapidly, so the present day period represents the initial one
- Then, the field of PSR 1852 was not enhanced via a dynamo mechanism
- Detection of millisecond "hidden" magnetars will be a strong argument in favour of dynamo.

1307.3127

A PULSAR WITH GROWING FIELD?

PSR J1734−3333
n=0.9+/-0.2

Will it become a magnetar?

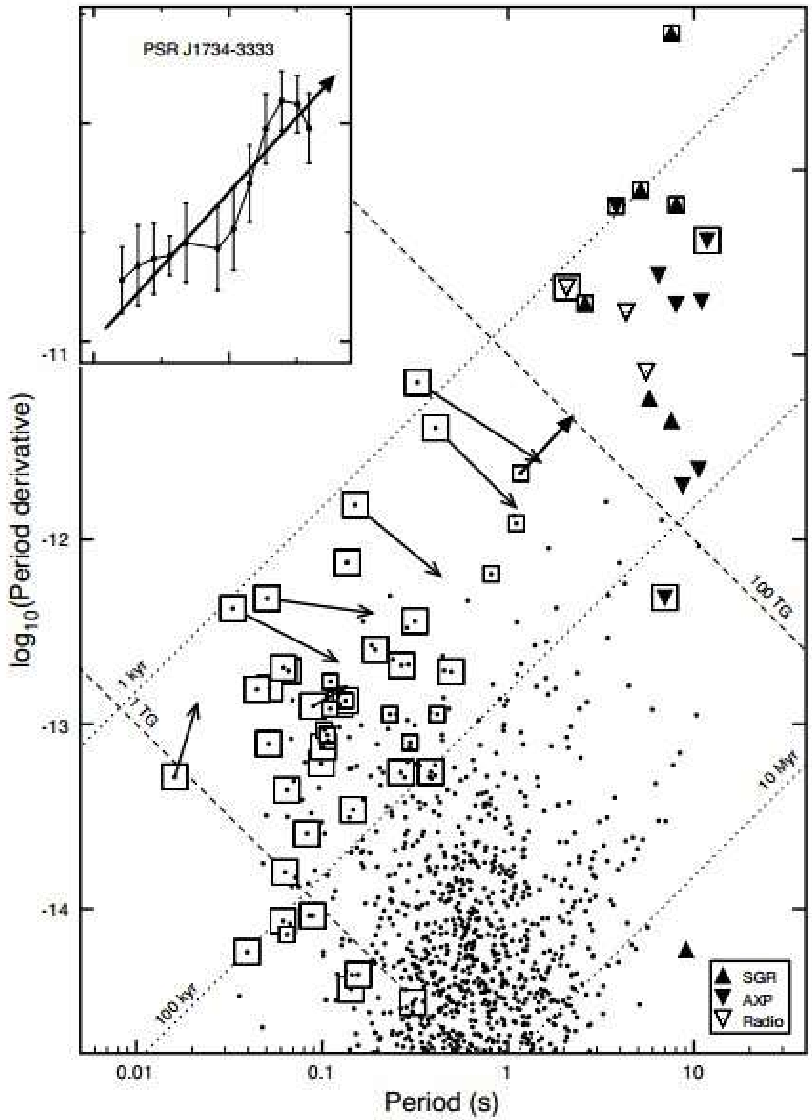

Espinoza et al. arXiv: 1109.2740

LOW-FIELD MAGNETARS

SGR 0418+5729, 3XMM J185246.6+003317 and Swift J1822.3–160

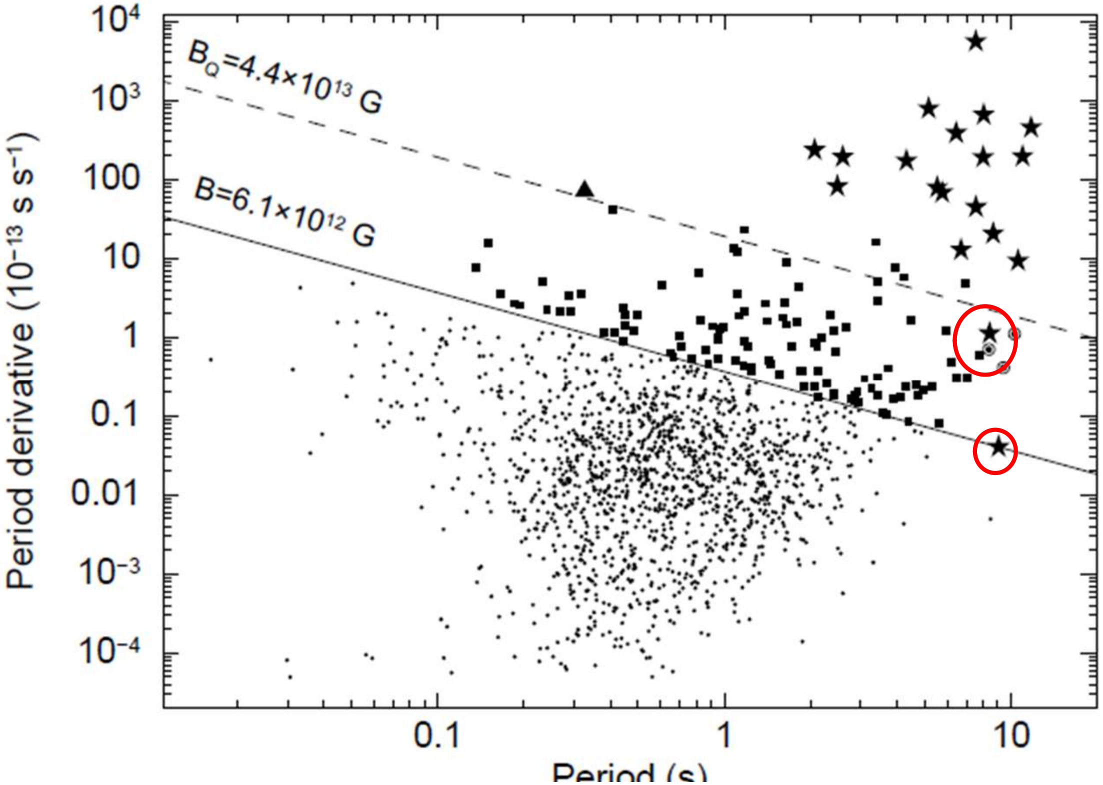

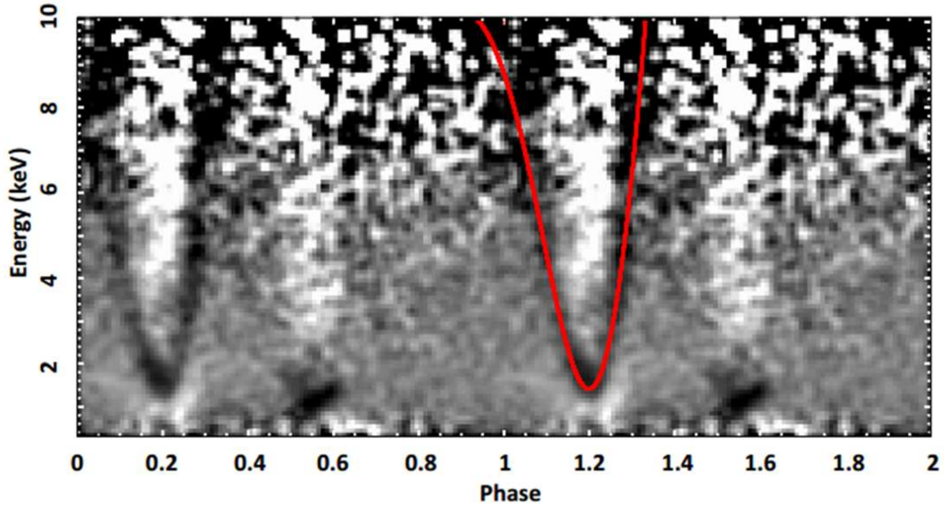

1308.4987

XMM-Newton observations allowed to detect a spectral line which is variable with phase.
If the line is interpreted as a proton cyclotron line, then the field is 2 10^{14} – 10^{15} G

NEW RECORDS:
76 SECONDS AND 18 MINUTES

PSR J0901−4046
76 seconds spin period

MeerKAT observations
(2206.01346)

GLEAM-X J162759.5-523504.3
~18 munites periodicity.
Nature is uncertain.

Murchison Widefield Array
(Hurley-Walker et al.)

Now this class of so-called
Long-Period Radio Transients
consists of more than a dozen sources.
Some are WD+RD binaries,
but some can be isolated NSs.

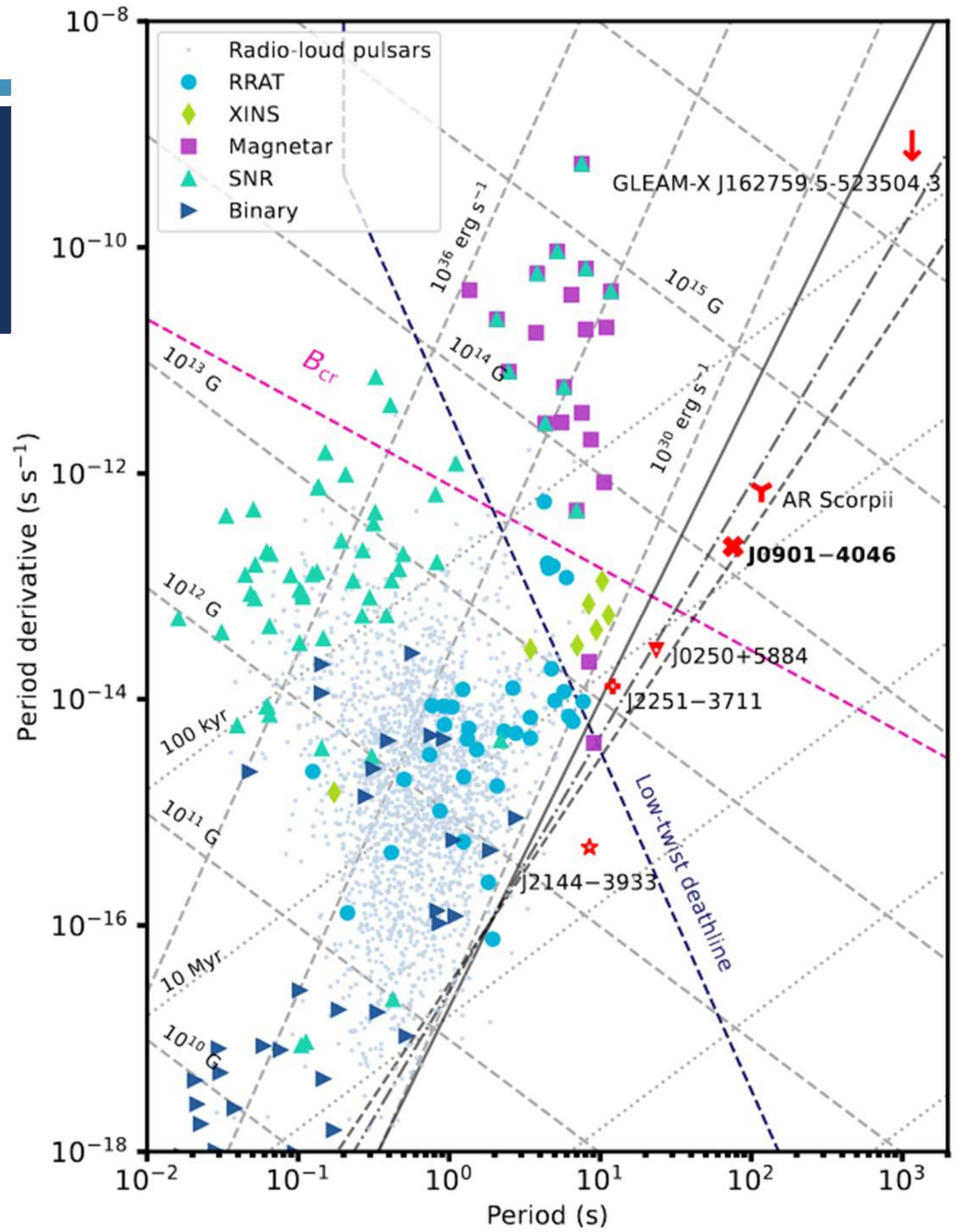

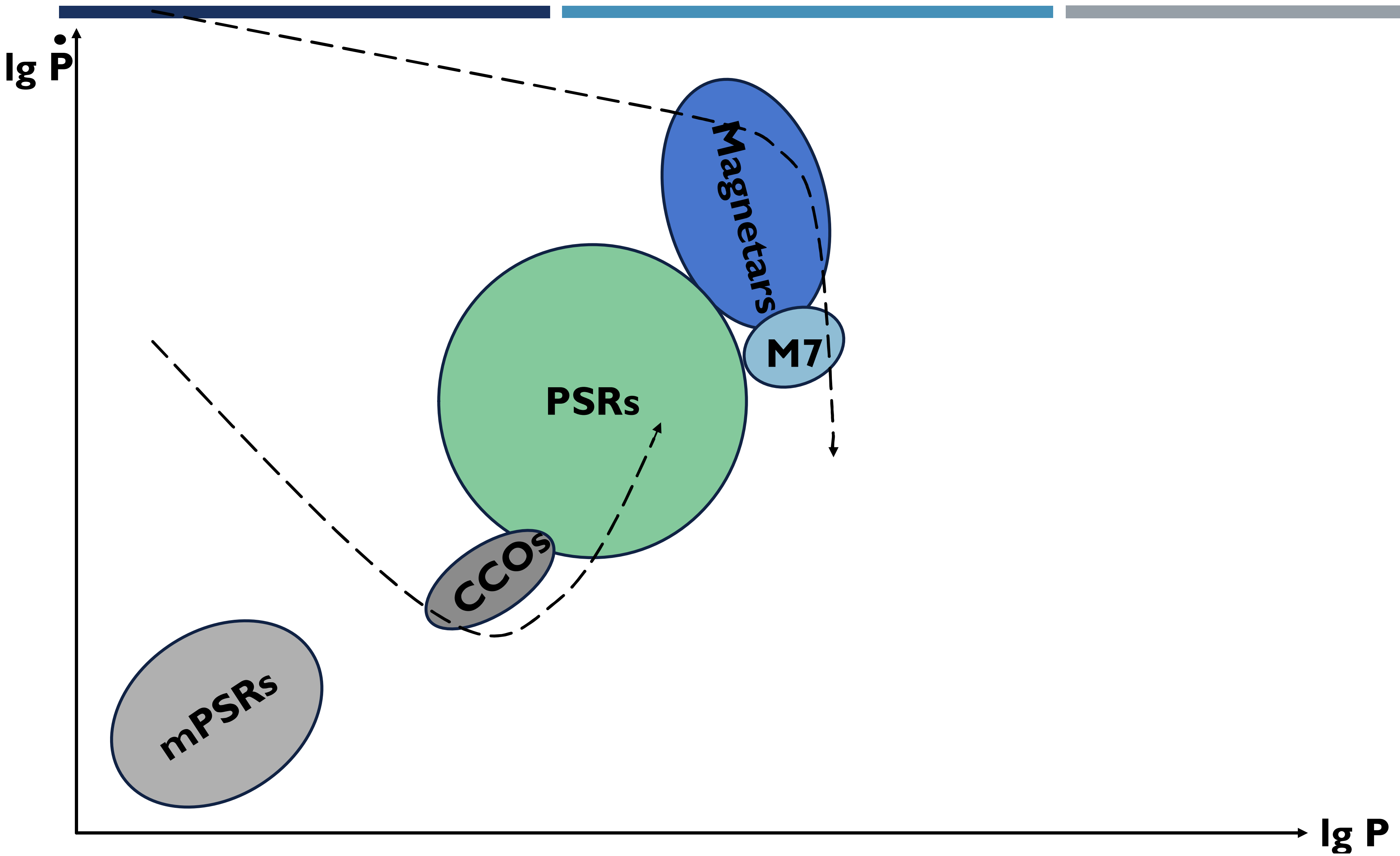
lg Ṗ
Magnetars
M7
PSRs
CCOs
mPSRs
lg P

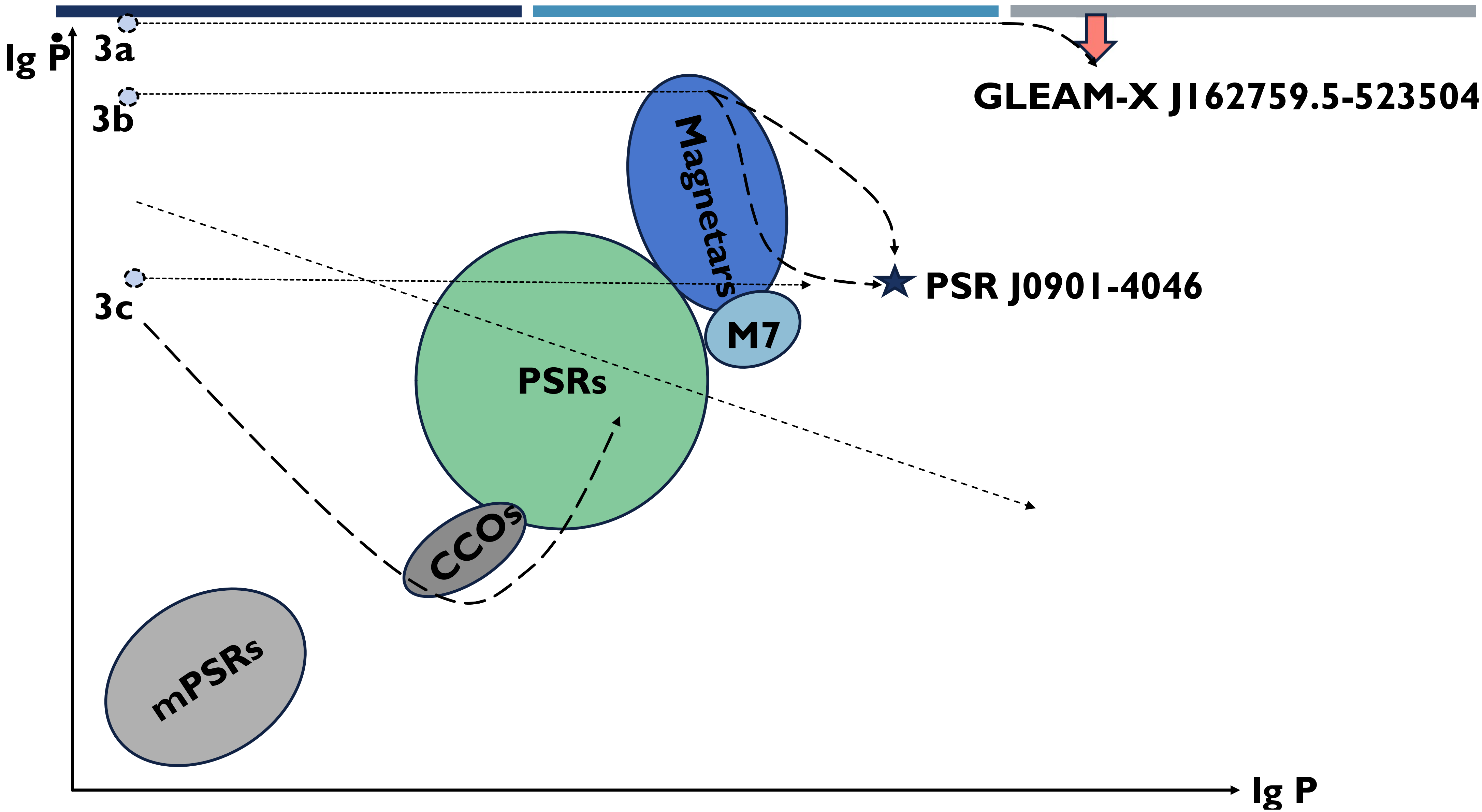
lg Ṗ
3a
3b
3c
GLEAM-X J162759.5-523504
Magnetars
PSR J0901-4046
M7
PSRs
CCOs
mPSRs
lg P

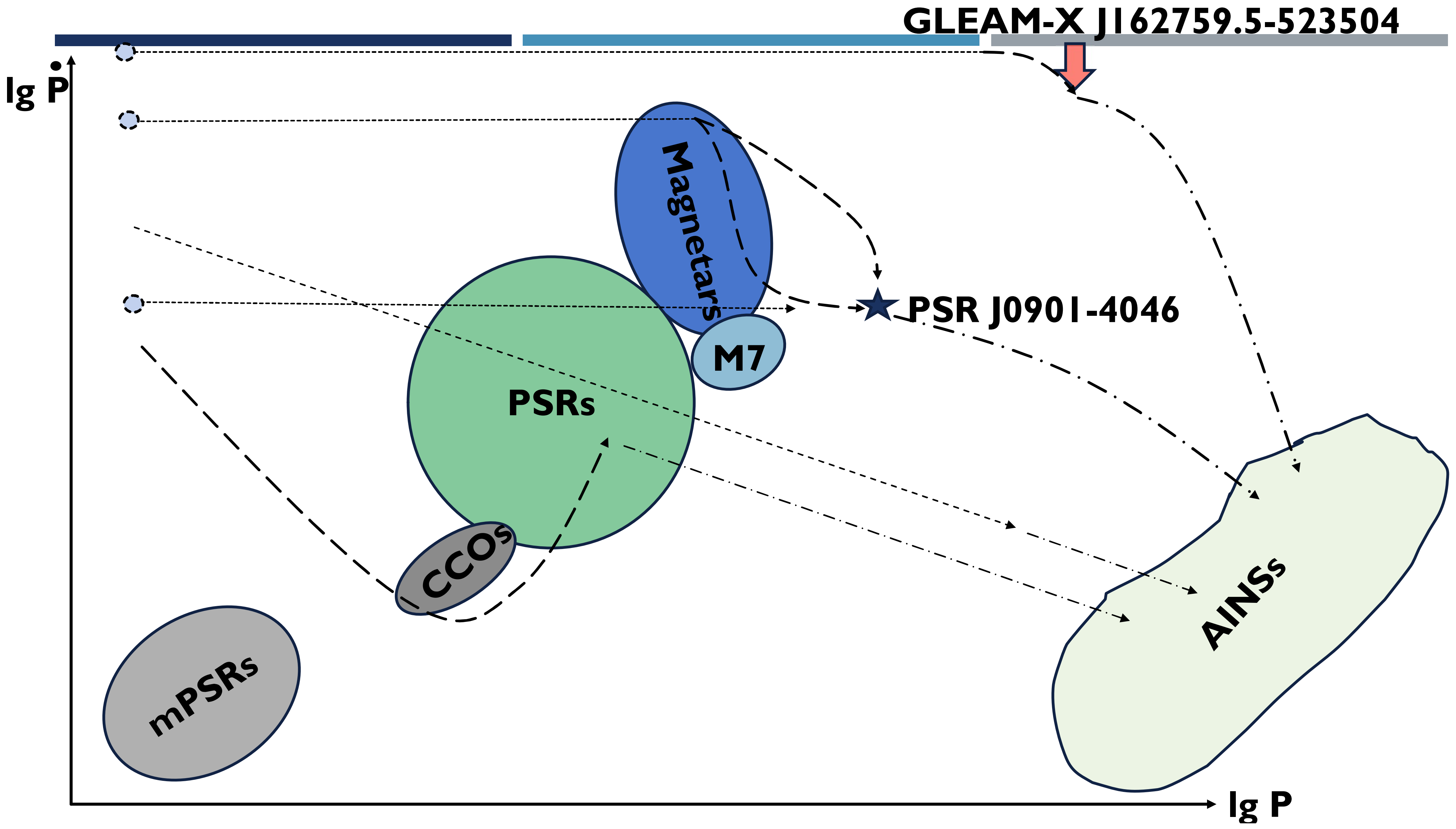

GLEAM-X J162759.5-523504
lg Ṗ
Magnetars
PSR J0901-4046
M7
PSRs
CCOs
AINSs
mPSRs
lg P

MAGNETARS AND FRBS: SGR 1935+2154

Discovered in 2014 (see, Israel et al. 2016).
P=3.25 sec
Distance ~7-12 kpc (2005.03517)
Intermediate flare (Kozlova et l. 2016)

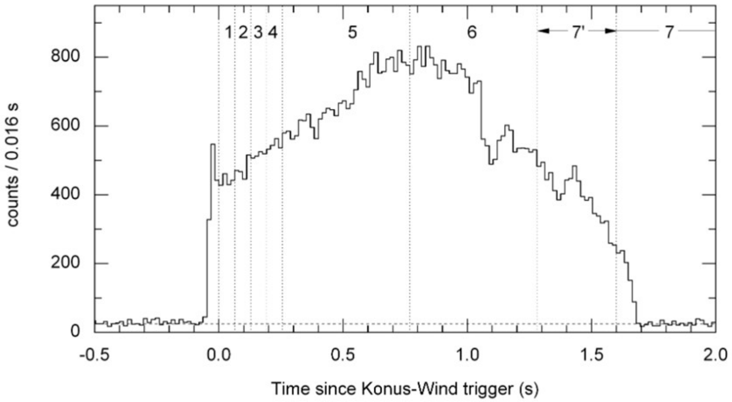

Activated in April 2020.
Finally, on April, 28 2020
a simultaneous burst in radio and
X/gamma has been detected.
In Oct. 2022 more bursts were detected.

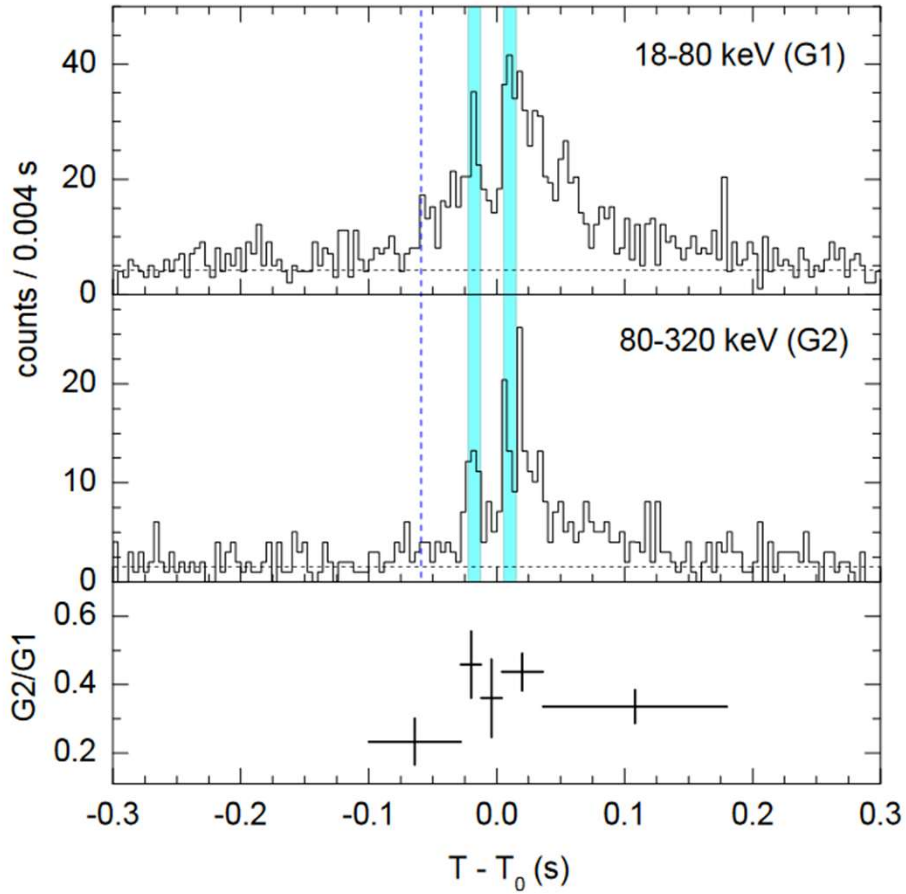

2005.11178

NEW POPULATION SYNTHESIS OF GALACTIC ISOLATED NSS

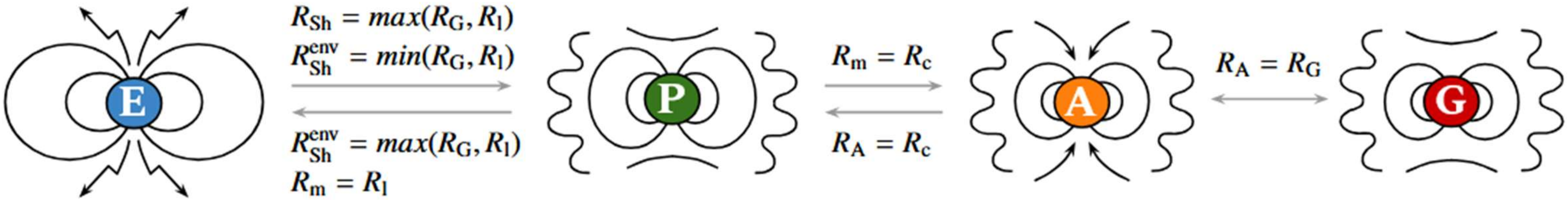

2512.10666

Main ingredients:

- Distribution of progenitors
- Galactic gravitational potential
- Interstellar medium properties
- Kick velocity
- Initial spin distribution of NSs
- Initial magnetic field distribution
- Magnetic field evolution
- Models of spin-down for Propeller
- Accretion regime

We use four models for the Propeller stage.

This is a crucial ingredient of our modeling as we aim to estimate the number of accreting isolated NSs.

Model	Braking torque $K_{\rm P}$
A	$\dot{M}\omega R_{\rm m}^2$
B	$\dot{M}\sqrt{2GMR_{\rm m}}$
C	$\dot{M}\max[v_\infty^2,\ v_{\rm ff}^2(R_{\rm m})]/(2\omega)$
D	$\dot{M}v_\infty^2/(2\omega)$

Model A is the most efficient, i.e. the Propeller stage is the shortest. Oppositely, for Model D the duration of the Propeller stage ca be very long. Thus, the number of Accretors is small in this scenario.

ACCRETORS

To become an Accretor, an NS might have either strong magnetic field or/and large initial spin period (less realistic).

Basically, this results remain unchanged for other models of the ISM, Propeller, and magnetic field evolution.

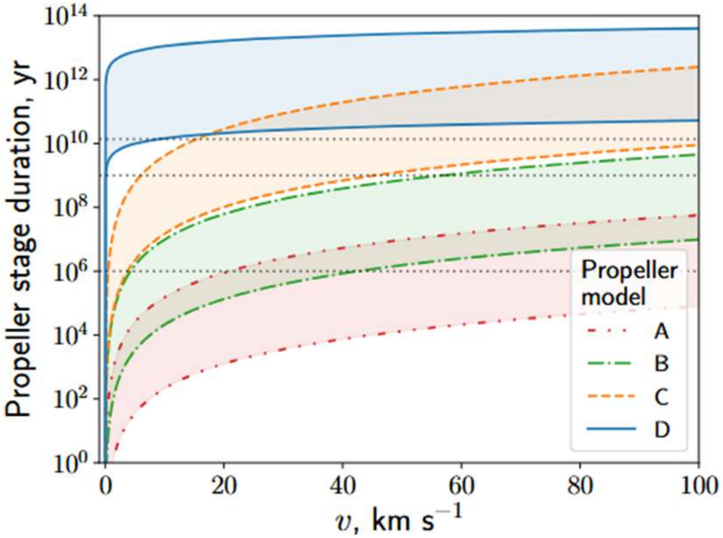

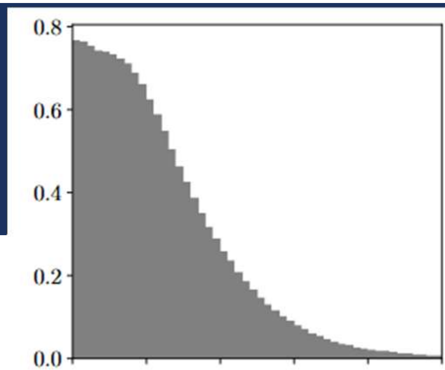

The results correspond to constant magnetic field, single-phase ISM model, and propeller model A (i.e., efficient propeller).

Calculations are done for uniform distribution in the initial parameters in order to illustrate the evolutionary trends.

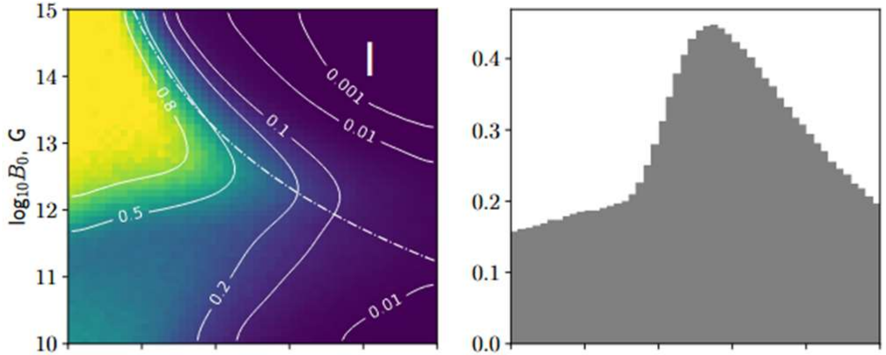

Color shows which fraction of its life an NS spends as an Accretor.

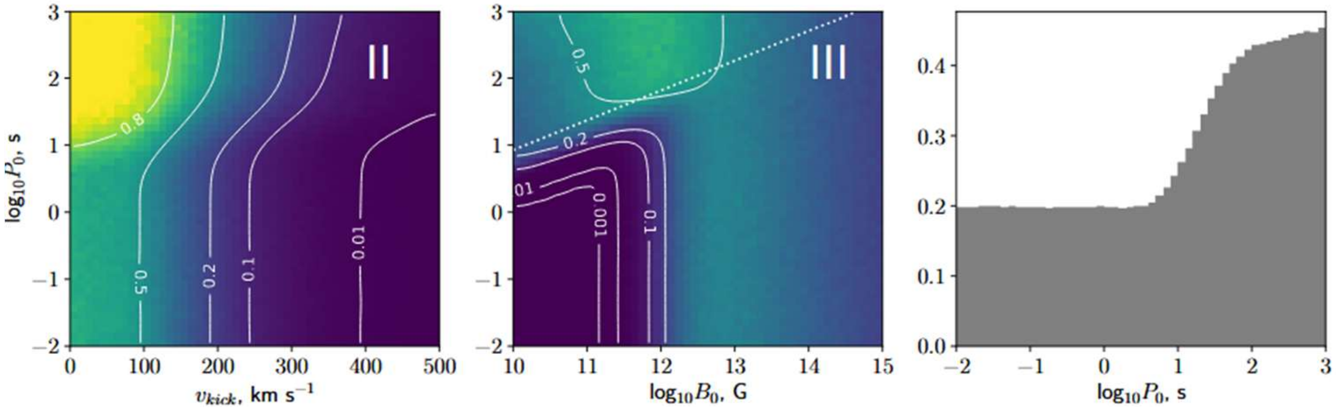

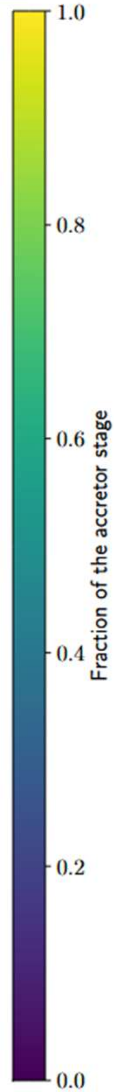

NSS IN VARIOUS STAGES OF EVOLUTION

We used four models for propeller spin-down, two models of the ISM, and two models for the magnetic field evolution.

In our opinion, the model with the two-phase ISM, exponentially decaying magnetic field, and propellers B or C are more realistic.

They predict a significant number of isolated Accretiors.

Two-phase ISM, constant field

Propeller model	Ejector	Propeller	Accretor
A	42.4 ± 0.7	6.53 ± 0.14	36.2 ± 0.4
B	60.8 ± 0.9	14.6 ± 0.5	23.6 ± 0.6
C	72.3 ± 1.1	26.2 ± 1.0	1.50 ± 0.14
D	73.0 ± 1.0	27.0 ± 1.0	$\sim 10^{-4} - 10^{-3}$

Two-phase ISM, exponentially decaying field

Propeller model	Ejector	Propeller	Accretor
A	18.42 ± 0.24	40.0 ± 0.4	41.3 ± 0.6
B	20.98 ± 0.26	61.7 ± 0.6	17.3 ± 0.7
C	21.96 ± 0.26	75.11 ± 0.19	2.93 ± 0.22
D	21.98 ± 0.25	78.02 ± 0.25	$\sim 10^{-4} - 10^{-3}$

In the Solar proximity, the fraction of Accretors is larger than on average, because the ISM density is larger than on average and most of old NSs around us have been born with relatively low spatial velocities (otherwise, they spend most of the lives out of the disc).

NUMBERS FOR EROSITA

Here we assume that the accretion rate is

$$\dot{M} = \pi R_G^2 \rho v = 4\pi (GM)^2 \rho v^{-3} =$$
$$= 7.3 \times 10^8 \left(\frac{n}{1\ \mathrm{cm}^{-3}}\right)\left(\frac{v}{100\ \mathrm{km\,s}^{-1}}\right)^{-3}\ \mathrm{g/s},$$

Two-phase ISM		
Propeller model	Constant field	Exponential decay
A	4000 ± 400	3470 ± 260
B	4000 ± 400	3350 ± 250
C	2100 ± 150	2360 ± 150

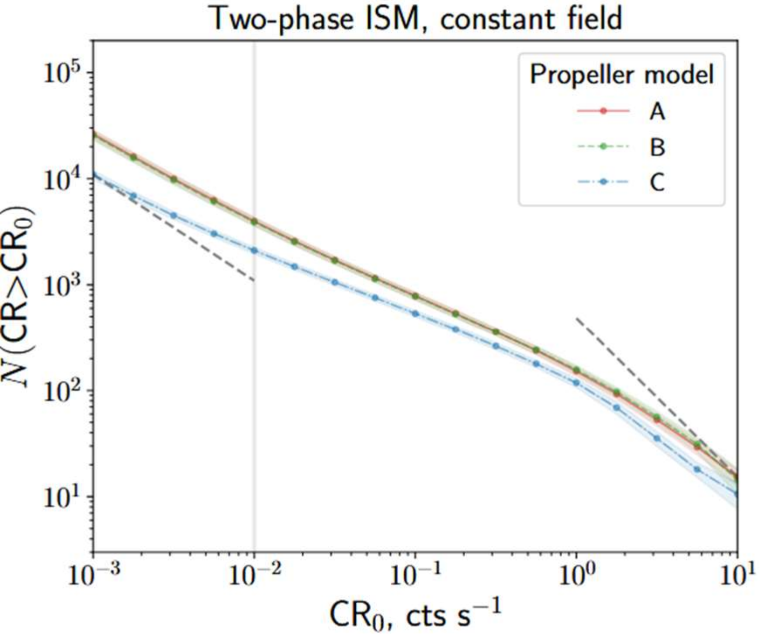

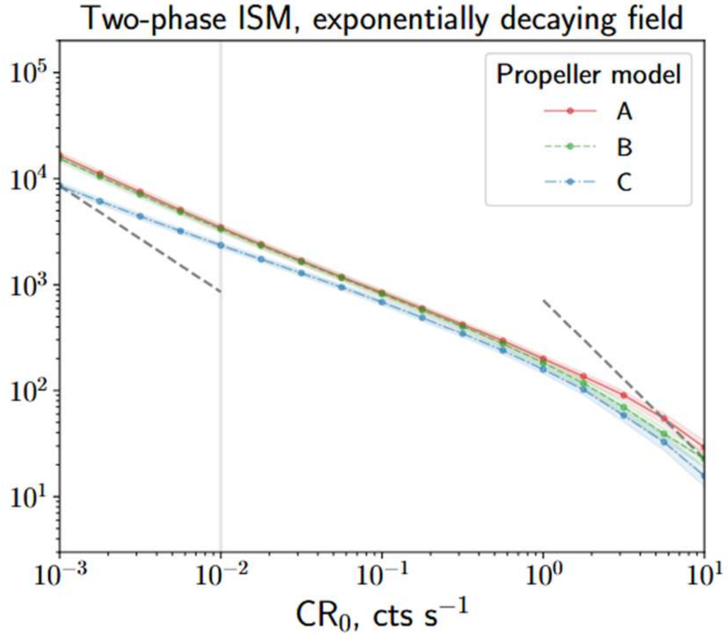

These predictions are quite optimistic. However, they must be taken with a grain of salt.

We are not sure about the regime of accretion in the case of isolated NS. At low rates, accretion can become less efficient or/and transient.

Spectral properties of isolated accretors are also uncertain.

CONCLUSIONS

- Variety of observational appearance of NSs
- Variety of initial properties
- Various evolutionary paths

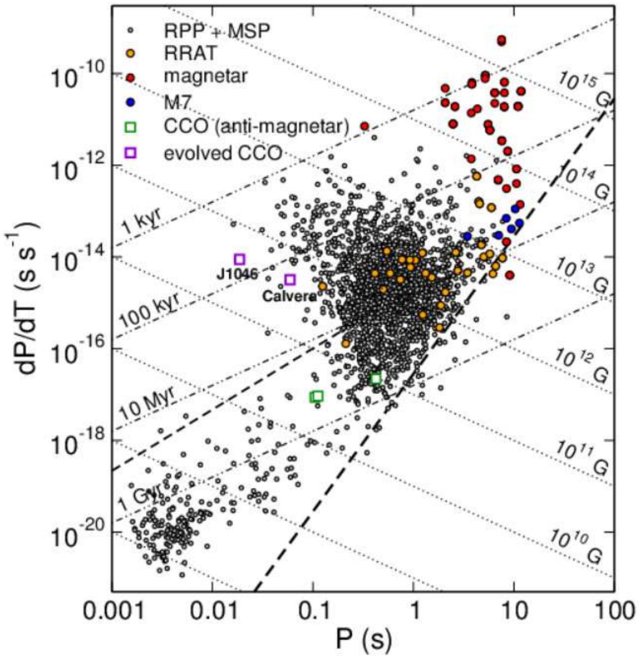

- Sources of double (triple) nature
- Examples of non-standard evolution
- Lack of understanding of evolution of many objects with non-standard parameters

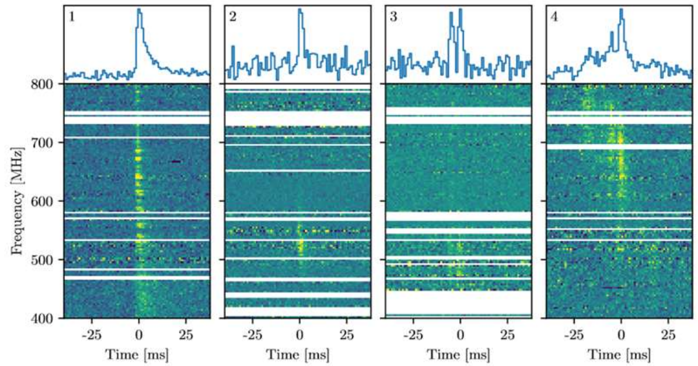

- Accreting isolated NS might be discovered soon. This will probe long-term evolution
- Dormant NSs in old binaries and microlensing also can give information about long-term evolution
- Soon sources of FRBs will outnumber all other known types of NSs in the next few years (2303.05591).